

Fermi National Accelerator Laboratory

FERMILAB-Pub-92/08-A
January 1992

DARK MATTER, LONG—RANGE FORCES, AND LARGE—SCALE STRUCTURE

BEN-AMI GRADWOHL AND JOSHUA A. FRIEMAN

NASA/Fermilab Astrophysics Center

Fermi National Accelerator Laboratory

P.O. Box 500, Batavia, IL 60510

ABSTRACT

If the dark matter in galaxies and clusters is non-baryonic, it can interact with additional long-range fields that are invisible to experimental tests of the Equivalence principle. We discuss the astrophysical and cosmological implications of a long-range force coupled only to the dark matter and find rather tight constraints on its strength. If the force is repulsive (attractive), the masses of galaxy groups and clusters (and the mean density of the universe inferred from them) have been systematically underestimated (overestimated). Such an interaction also has unusual implications for the growth of large-scale structure: a repulsive (attractive) force relatively enhances (suppresses) the growth of density perturbations on large scales and automatically generates a bias (antibias) between baryonic and non-baryonic matter. We explore the consequent effects on the two-point correlation function, large-scale velocity flows, and microwave background anisotropies, for models with initial scale-invariant adiabatic perturbations and cold dark matter.

Subject headings: cosmology — early universe — galaxies: clustering



1. Introduction

The observed flat rotation curves of galaxies and the application of the virial theorem to clusters of galaxies have revealed the presence of large amounts of dark matter, constituting perhaps 90% of the total mass in these systems. Several lines of argument suggest that much of the dark matter in galaxies and clusters is not baryonic (*e.g.*, Hegyi and Olive 1986), while particle physics models provide a gallery of exotic elementary particles as dark matter candidates (for a review, see Primack, Seckel, and Sadoulet 1988).

In keeping with the principle of equivalence, it is generally assumed that the dark matter gravitates like the visible baryons, *i.e.*, that it is subject only to gravitational forces. However, since the existence of dark matter is inferred solely from its gravitational effects, and its nature is otherwise unknown, this assumption is open to question. Although a new long-range force of gravitational strength coupled to *baryonic* matter is experimentally ruled out by the spate of recent ‘fifth-force’ experiments (for reviews, see Fackler and Tran Thanh Van 1989), there may be an additional long-range interaction which couples to a quantum number carried exclusively by *non-baryonic* matter (*e.g.*, one of the lepton flavors). Such an additional force clearly evades laboratory tests of the Equivalence principle. Its effects would only be manifest in systems where the dark matter is dynamically important, that is, in the outer regions of galaxies and in clusters. In this paper, we investigate the implications of additional long-range forces acting between non-baryonic dark matter particles (see also Frieman and Gradwohl 1991).

Long-range interactions have been proposed in the context of a variety of particle physics models. For example, in extended supergravity models (Scherk 1980), a vector field coupling to particles of mass m and effective charge $\sim m/m_{pl}$ gives rise to a repulsive force of gravitational strength (here $m_{pl} = G_N^{-1/2} = 1.2 \times 10^{19}$ GeV is the Planck mass, and throughout we use units in which $\hbar = c = 1$). Compactification of higher dimensional theories can also yield new vector and scalar forces of gravitational strength (Bars and Visser 1986). Alternatively, ultralight pseudo-Nambu-Goldstone bosons with scalar couplings, called *schizens* (cousins of Majorons and familons), can arise naturally in extensions of the standard electroweak model (Hill and Ross 1988).

As a concrete example, consider the phenomenological schizon model with Lagrangian

$$L = \bar{\psi} i \gamma_\mu \partial^\mu \psi + m_\psi \bar{\psi} \psi + \frac{1}{2} \partial_\mu \phi \partial^\mu \phi + \frac{\epsilon}{f} \phi \bar{\psi} \psi - \frac{1}{2} m_\phi^2 \phi^2, \quad (1.1)$$

where the fermion ψ of mass $m_\psi \sim 1 - 10$ eV constitutes the dark matter ($\Omega_\psi \simeq 1$), ϕ is the schizon, and f is a global symmetry breaking scale. For a static configuration, the

scalar field satisfies a modified Poisson equation,

$$\nabla^2 \phi - m_\phi^2 \phi = \frac{\epsilon}{f} \langle \bar{\psi} \psi \rangle \quad (1.2)$$

In the non-relativistic limit, the fermion density $n_\psi = \langle \bar{\psi} \psi \rangle$, and the static potential between two separated fermion sources with masses M_1 and M_2 has the Yukawa form,

$$V_\phi = -\frac{\epsilon^2}{4\pi m_\psi^2 f^2} \frac{M_1 M_2}{r} e^{-m_\phi r}. \quad (1.3)$$

Thus, on scales $r \ll m_\phi^{-1}$, the relative magnitude of the scalar force is $\alpha = G_\phi/G_N = \epsilon^2 m_{pl}^2 / m_\psi^2 f^2$; for $\epsilon \sim m_\psi$ and $f \sim m_{pl}$ it has roughly gravitational strength. In these models the scalar mass is of order $m_\phi \sim \epsilon m_\psi / f$, so the range of the attractive force is astronomical, $\lambda = m_\phi^{-1} \simeq 100 \alpha^{-1/2} (\text{eV}/m_\psi)^2 \text{ kpc}$.

As an aside, we make two comments regarding this model. First, the phase space constraint on fermion clustering (Tremaine and Gunn 1979) applied to dwarf spirals suggests that a light fermion constituting the dark matter in galaxy halos should be somewhat heavier than above, $m_\psi \gtrsim 100 \text{ eV}$ (*e.g.*, Spergel, Gott, and Weinberg 1989). Since typically $\Omega_\psi h^2 \simeq (m_\psi/90) \text{ eV}$ (where the Hubble parameter $H_0 = 100h \text{ km/sec/Mpc}$), this requires entropy production after the fermions drop out of thermal equilibrium in the early universe, in order to satisfy constraints from the age and expansion rate of the universe, $\Omega h^2 \leq 1$. For neutrinos this is difficult to arrange without adversely affecting big bang nucleosynthesis (but not impossible — see Scherrer, Cline, Raby, and Seckel 1991); however, other more weakly coupled fermions may freeze out earlier, *e.g.*, before the quark-hadron transition, and have their cosmic density substantially diluted. Since $\lambda \sim m_\psi^{-2}$, a heavier dark matter fermion implies a reduction in the range of the scalar force. Second, we note that the schizon model naturally incorporates galactic-range forces if the dark matter is a *light* fermion. Unless the fermions have additional interactions which reduce their mean free path and thus prevent free streaming (Raffelt and Silk 1987), this suggests we consider such a force in the context of hot dark matter models for structure formation. However, in other particle physics models, one can contemplate long range forces between cold dark matter particles as well.

Regardless of the particle physics origin of such a force, in general the potential energy of two non-baryonic masses M_1 and M_2 at separation r may be parameterized by

$$V(r) = -G_N \frac{M_1 M_2}{r} (1 + \alpha e^{-r/\lambda}), \quad (1.4)$$

where the range of the additional interaction is fixed by the Compton wavelength of the

exchanged vector ($\alpha < 0$) or scalar ($\alpha > 0$) particle, $\lambda = 1/m_{\nu,s}$. The resulting force is

$$F(r) = -\frac{G_N M_1 M_2}{r^2} [1 + \alpha(1 + r/\lambda)\exp(-r/\lambda)]. \quad (1.5)$$

We will study the astrophysical implications of and constraints upon the relative force strength α for a range of wavelengths λ . Since there are gravitationally bound systems dominated by dark matter, we can immediately infer that $\alpha > -1$ for $\lambda \gtrsim 10$ kpc. In Section II, we consider constraints on additional forces arising from the dynamics of galaxies, groups, and clusters. In Section III, we explore long-range forces in cosmology and consider in detail their effects on the linear growth of density perturbations and the formation of large-scale structure. In particular, assuming an initial spectrum of adiabatic perturbations with cold dark matter, we estimate the modification of the transfer function for perturbations due to a long-range interaction and the corresponding consequences for microwave background anisotropies, large-scale peculiar velocities, and the two-point galaxy correlation function. We also consider a final constraint on α arising from the response of dark halos to dissipational baryonic infall in the early stages of galaxy formation. We conclude in Section IV.

Tests of the Equivalence principle have been previously discussed for specific particles. The experimental bound (Fackler and Tran Thanh Van 1989) from Eötvös-type experiments on intermediate-range forces between baryons is approximately $|\alpha_b| \lesssim 10^{-4}$. In addition, supernova 1987a has been used to test for additional galactic-range forces coupling to electron neutrinos (Pakvasa, Simmons, and Weiler 1989 and references therein). By contrast, while we will assume that the dark matter on halo and cluster scales is composed of non-baryonic particles, the constraints we will consider are independent of the identity of these particles. For completeness, we note that the cosmological effects of an exactly massless Jordan-Brans-Dicke scalar field which couples with different strengths to ‘visible’ and ‘invisible’ matter has been discussed by Damour, Gibbons, and Gundlach (1990).

2. Constraints on Long-range forces from Galaxy and Cluster Dynamics

Given the theoretical models and experimental constraints above, we now consider the astrophysical effects of a long-range force coupled only to non-baryonic dark matter. We parameterize the mass density in terms of the mass-to-light ratio in the V band, $\Upsilon = \langle M/L \rangle_V$. From the observed mean luminosity density $j_V = (1.7 \pm 0.6) \times 10^8 h L_\odot \text{Mpc}^{-3}$ (e.g., Davis and Huchra 1982, Kirshner, *et al.* 1983), the cosmic density parameter can be expressed as $\Omega = 6 \times 10^{-4} h^{-1} \Upsilon / \Upsilon_\odot$. Thus, the critical mass-to-light ratio for an $\Omega = 1$ universe is $\Upsilon_c = (1600 \pm 500) h \Upsilon_\odot$. Clearly a long-range interaction of strength comparable to gravity will affect dynamical estimates of the masses of gravitationally bound systems and thus the value of Ω inferred from them.

First consider individual galaxies. The observation of high proper motion stars in the solar neighborhood (presumably bound to the Galaxy) implies that the local value of the galactic escape velocity exceeds 450–500 km/sec (Carney and Latham 1987; Cudworth 1990; Leonard and Tremaine 1990; for a review, see Fich and Tremaine 1991). In a truncated isothermal sphere model, this implies that the total mass-to-light ratio for the Milky Way is at least $\Upsilon_{MW} \gtrsim 30 \Upsilon_\odot$. This is consistent with the results obtained by requiring that distant globular clusters and satellite galaxies are bound to the Galaxy, as well as with mass-to-light ratios inferred from flat rotation curves in other spiral galaxies (Binney and Tremaine 1987; Fich and Tremaine 1991). Dynamical measurements of the mass within galaxies rely on baryonic tracers (stars or gas) of the gravitational potential. Since we assume that the new interaction does not couple to baryons, the masses inferred for individual galaxies, $M_{\text{inf}}(r) \sim v^2 r / G_N$, are the true masses, i.e., they are independent of α .

In systems of galaxies, however, such as binaries, groups, and clusters, galaxies themselves are used as test particles. If the galaxy mass is dominated by non-baryonic dark matter, one must take into account the additional force on the dark mass. Consider two galaxies in a binary system with separation $r \ll \lambda$, approaching each other with relative speed v_r ; from Kepler's law

$$r v_r^2 \propto G_N M_{\text{inf}} = G_N [1 + \alpha(1 - F)] M_{\text{true}} , \quad (2.1)$$

where M_{true} is the true (luminous plus dark) mass of the binary system, M_{inf} is the mass one erroneously infers without knowledge of the additional force, and $F = M_b / M_{\text{true}}$ is the baryon mass fraction of the system. Thus, the dynamical estimate of the cosmic mass

density satisfies

$$\frac{\Omega_{\text{true}}}{\Omega_{\text{inf}}} = \frac{\Upsilon_{\text{true}}}{\Upsilon_{\text{inf}}} = \frac{1}{1 + \alpha(1 - F)}. \quad (2.2)$$

A repulsive force ($\alpha < 0$) would delude us into believing that the dark matter density is smaller than it actually is. For example, a spatially flat universe with $\Omega_{\text{true}} = 1$ could masquerade as an open universe with $\Omega_{\text{inf}} < 1$, perhaps reconciling the theoretical prejudice for a flat universe with the observational indications on scales of groups and clusters that $\Omega_{\text{inf}} \lesssim 0.2 - 0.3$. Although an intriguing possibility, we show below that the value of α required, $\alpha \simeq -0.75$, is inconsistent with cluster observations.

To first approximation, the Local Group of galaxies can be thought of as a binary system, dominated by our Galaxy and Andromeda (M31), with a separation $r \simeq 725$ kpc. The two galaxies are approaching each other at relative speed $v_r = 123$ km/sec. Assuming the orbit is radial, eq. (2.1) implies (Binney and Tremaine 1987, and references therein) $\Upsilon_{\text{inf}}(\text{LG}) = 76 - 130\Upsilon_{\odot}$. (The range arises from the factor of two uncertainty in the age of the universe, $t_0 = (1 - 2) \times 10^{10}$ yr.) Since M31 is expected to have a ratio of dark to luminous matter and a stellar population similar to those of the Milky Way, and assuming M/L is a non-decreasing function of scale, the true mass-to-light ratio of the Local Group should at least equal that of our galaxy, $\Upsilon_{\text{true}}(\text{LG}) \gtrsim 30\Upsilon_{\odot}$. From eq. (2.2) this implies the approximate upper bound $\alpha \lesssim 4 \exp(700 \text{ kpc}/\lambda)$. Allowing for tidal torquing and mass infall in the Local group does not substantially alter this bound (Fich and Tremaine 1991 and references therein).

So far, we have implicitly assumed that the luminous baryons are gravitationally enslaved to their dark halos. In the core of a rich cluster, the outer halos of most galaxies are thought to be tidally stripped off by the cluster potential (Merritt 1984, Pryor and Geller 1984), and there is some observational evidence for this effect (Whitmore, Forbes, and Rubin 1988, Bothun and Schombert 1988, Lauer 1988); farther out, at distances $R \gtrsim 1h^{-1}$ Mpc from the center of a typical rich cluster, the halos of galaxies appear to be relatively intact, in the sense that spirals with extended flat rotation curves are found there. Now, if $\alpha \neq 0$ an additional *non-tidal*, bulk stripping force arises from the fact that the orbital speeds of the baryonic core and the dark halo of a galaxy (each treated as test particles) *at the same point* in the field of a central mass M (another galaxy or a cluster) do not coincide. If α is very large, bulk stripping could conceivably lead to the complete separation of baryonic disks from their non-baryonic halos. If α is only moderately large, bulk stripping is counterbalanced by the mutual gravitational attraction between the disk and the halo. In this case, a spiral disk in a cluster would be displaced from the center of mass

of its halo, and its rotation curve would presumably be asymmetric; in addition, the disk itself could be warped.

To estimate the magnitude of this effect, consider the following idealized system: a rich, spherical cluster, centered at the origin, with mass $M_{cl}(r)$, a spherical, non-baryonic galaxy halo, with center of mass coordinate $\vec{r}_h(t)$, central density ρ_h , and core radius r_c , and a point-like baryonic core, with negligible dynamical mass, at coordinate $\vec{r}_b(t)$. We neglect the gravitational backreaction of the galaxy halo and core on the cluster, *i.e.*, we treat the cluster potential as fixed. In order to ensure that the rotation curve is not noticeably asymmetric, we assume the displacement between the core and halo must be small compared to the halo core radius, $\Delta = |\vec{r}_b - \vec{r}_h| \ll r_c$ (but see below). For galaxies farther than a few kpc from the cluster center of mass, this implies $\Delta \ll |\vec{r}_b|, |\vec{r}_h|$. The first inequality above means that the halo restoring force on the baryonic core is determined completely by ρ_h and Δ , while the second inequality implies that the cluster masses interior to the instantaneous core and halo orbits are essentially identical, $M_{cl}(r_b) \simeq M_{cl}(r_h)$ (corrections to this approximation enter at next order in Δ/r_h).

Consider the galaxy core and halo on radial orbits through the cluster, with instantaneous radii $r_b = r_h + \Delta$ and r_h . To lowest order in Δ/r_h , the core-halo separation satisfies

$$\ddot{\Delta} + \frac{4\pi}{3}G_N\rho_h\Delta = G_N M_{cl}(r_h) \left[\frac{1+\alpha}{r_h^2} - \frac{1}{(r_h+\Delta)^2} \right] \quad (2.3)$$

For $\alpha = 0$, the term in brackets represents the usual tidal force, and the equilibrium displacement between the core and halo vanishes, $\Delta = 0$. Assuming equilibrium is established on a timescale short compared to the crossing time through the cluster, for $\alpha \neq 0$ the equilibrium displacement between the core and halo is

$$\frac{\Delta}{r_h} \simeq \alpha \left(\frac{\rho_h}{\bar{\rho}_{cl}(< r_h)} - 2 \right)^{-1} \quad (2.4)$$

where $\bar{\rho}_{cl}(< r)$ is the mean cluster density interior to radius r .

As an example, consider a typical spiral galaxy $r_h = 1$ Mpc from the center of the Coma cluster. The estimated cluster mass interior to this radius is approximately $M_{Coma}(1 \text{ Mpc}) \simeq 6 \times 10^{14} M_\odot$, and this appears to be robust against assumptions about velocity anisotropy, variations in M/L , etc. (Merritt 1987); thus, $\bar{\rho}_{Coma}(< 1h^{-1} \text{ Mpc}) \simeq 1.4 \times 10^{-4} M_\odot \text{ pc}^{-3}$. This is well below typical estimates for spiral halo densities; *e.g.*, for the Sc galaxy NGC 3198, the rotation curve can be fit with central density $\rho_h = (0.013 - 0.58)h^2 M_\odot \text{ pc}^{-3}$, with corresponding halo core radii in the range $r_c = (6.4 - 1.1)h^{-1} \text{ kpc}$

(van Albada *et al.* 1985). (We note that the important parameter $\rho_h r_c^2$ is essentially fixed by the observed rotation speed, and is independent of α .) To good approximation, we therefore find $\Delta/r_h \simeq (\bar{\rho}_{cl}(< r_h)/\rho_h)\alpha$. Spanning the range from maximum to minimum disk models, if NGC 3198 were placed 1 Mpc from the center of Coma it would satisfy $\Delta/r_c = (0.2 - 1.6)h^{-2}\alpha$. Requiring this ratio to be less than unity, we obtain the bound $|\alpha| \lesssim 5$ (where we have taken $h = 1$ to obtain a conservative limit). We caution, however, that without detailed modelling we do not know how reliable this bound is: since rotation curves are flat and relatively featureless beyond a few disk scale lengths, the precise signature of the asymmetry is not obvious. (In cases where the disk is dynamically significant, presumably a feature would arise in the rotation curve at the point where the halo begins to dominate over the disk; for a different aspect of this problem, see section 3.6 below.)

Two strong constraints on the interaction strength α for ranges $\lambda \gtrsim 1$ Mpc arise from the dynamics of rich clusters. The first involves the distribution of hot intracluster gas (for recent reviews, see Sarazin 1988, Oegerle, Fitchett, and Danly 1990). If the gas is isothermal and in hydrostatic equilibrium in the potential well of a spherical cluster with mass profile $M(r)$, then

$$\frac{1}{\rho_{gas}} \frac{d\rho_{gas}}{dr} = \frac{k_B T_{gas}}{\mu m_p} \frac{d \ln \rho_{gas}}{dr} = -\frac{G_N M(r)}{r^2}, \quad (2.5)$$

where μ is the gas mean molecular weight in *amu*, and m_p is the proton mass. Similarly, if the cluster galaxies have an isotropic, spatially constant, one-dimensional velocity dispersion σ , then

$$\sigma^2 \frac{d \ln \rho_{gal}}{dr} = -\frac{G_N M(r)}{r^2}. \quad (2.6)$$

Equating eqs. (2.5) and (2.6), the gas density satisfies (Cavaliere and Fusco-Femiano 1976)

$$\rho_{gas}(r) \propto \rho_{gal}(r)^{\beta_s}, \quad (2.7)$$

where

$$\beta_s \equiv \frac{\sigma^2 \mu m_p}{k_B T_{gas}}. \quad (2.8)$$

The observed surface density profile for galaxies in a cluster is generally reproduced by a King model, with

$$\rho_{gal} \propto [1 + (\tau/r_c)^2]^{-3/2}. \quad (2.9)$$

From X-ray surface brightness observations, most clusters are well fit by the gas density

profile

$$\rho_{gas}(r) = \rho_0[1 + (r/r_c)^2]^{-3\beta_f/2}, \quad (2.10)$$

with $\beta_f = 0.6 - 0.8$ (Jones and Forman 1984). We thus expect $\beta_s = \beta_f$ if galaxies trace the cluster mass. However, observations of the X-ray spectral temperatures and the galaxy velocity dispersion of a number of clusters imply (Mushotsky 1984) $\beta_s \simeq 1.2 \simeq 2\beta_f$; this difference is known as the β -discrepancy.

In the presence of a long-range force, if most cluster galaxies retain their dark halos (and therefore orbit the cluster as dark matter particles), eq. (2.6) is modified by replacing $G_N \rightarrow G_N[1 + \alpha(1 - F)]$. This implies

$$\beta_s(\alpha) = \frac{\beta_s(\alpha = 0)}{1 + \alpha(1 - F)}. \quad (2.11)$$

Thus, the discrepancy would be resolved (*i.e.*, $\beta_s(\alpha) \simeq \beta_f$) if $\alpha \simeq 1$. However, the ‘ β -problem’ is most likely a reflection of the simplified assumptions used above (Sarazin 1988, Fitchett 1990, Evrard 1990) rather than a signal of new physics. For example, the gas may not be isothermal, galaxies may not faithfully trace the mass, the galaxy velocity dispersion σ may be anisotropic and/or a function of radius, and the King model may be a poor fit at large radii. Instead, we can use the factor of 2 agreement between the two determinations of β to place constraints on α . For the ensemble of cluster observations, we have approximately $1 \lesssim \beta_s(\alpha = 0)/\beta_f \lesssim 2$. Naively, we would expect $\beta_s(\alpha) = \beta_f$, but the corrections cited above generally go in the direction of increasing β_s/β_f from unity, and can adequately explain the β -discrepancy (Evrard 1990). We therefore expect on theoretical grounds $1 \lesssim \beta_s(\alpha)/\beta_f \lesssim 2$. Using eq. (2.11) with $F \lesssim 0.2$, we then obtain the bound $-0.6 \lesssim \alpha \lesssim 1.3$.

An independent bound on α comes from the giant luminous arcs, high redshift galaxies gravitationally lensed by foreground galaxy clusters (Lynds and Petrosian 1986; Soucail, *et al.* 1987; for a review, see Mellier, *et al.* 1990). These arcs are formed when a galaxy is nearly imaged into an Einstein ring. Assuming photons do not couple to the new force (they are deflected only by the gravitational potential), from the observed lensing geometry one can estimate the true cluster mass interior to the radius of the arc. Comparison with the dynamically inferred cluster mass obtained from the virial theorem, which is sensitive to the additional force, yields a constraint on α comparable to that above.

The most useful cluster for our purposes appears to be Abell 370. Using the measured redshifts for the lensed galaxy, $z_{arc} = 0.724$, and the lensing cluster, $z_c = 0.374$, Soucail,

et al. (1988) estimate the cluster mass $M(< r) \simeq (1.9 \pm 0.4) \times 10^{14} h_{50}^{-1} M_{\odot}$ over the scale $r < 150 h_{50}^{-1}$ kpc, where the Hubble parameter $H_0 = 50 h_{50}$ km/sec/Mpc. This corresponds to a mass-to-light ratio $(M/L)_R \simeq (100 \pm 25) h_{50}$ on this scale, where subscript R denotes the red band. The same group has also measured velocities for galaxies in the cluster and inferred a virial mass. For Abell 370, Mellier, *et al.* (1988) report $(M/L)_R = 56 \pm 15$ (again for $h_{50} = 1$) based on a line of sight velocity dispersion $\sigma = 1340$ km/sec obtained from 29 galaxy spectra; this value for the velocity dispersion is consistent with the results of Henry and Lavery (1987) for the same cluster, but the resulting virial estimate of M/L is almost a factor of two below the arc estimate. However, in a more recent proceedings (Moran, *et al.* 1988), Soucail reports that their measured velocity dispersion is $\sigma = 1700 \pm 170$ km/sec based on 46 velocity measurements. This yields the virial estimate $(M/L)_R = 96 \pm 10$, in much better agreement with the arc estimate.

One must use some care in comparing these two numbers: the arc value gives the mass-to-light ratio averaged over a tube extending along the line of sight through the cluster, with tube radius given by the (rather small) radius of curvature of the arc; on the other hand, the virial estimate uses galaxy velocities which extend considerably further out, and it assumes that the observed galaxies accurately trace the cluster mass (*i.e.*, constant M/L). Moreover, Merritt (1987) has shown that models with radially varying mass-to-light ratios are consistent with the galaxy position and velocity data in the much better studied Coma cluster (with several hundred measured velocities). Nevertheless, he shows that the constant M/L assumption gives a fairly reliable indicator of the mass in the *core* of the cluster; for Coma, he estimates that the true mass within 1 Mpc is within 25% of the virial estimate. Now, for Abell 370, we are interested in a smaller region, but the velocity data is more sparse. We therefore roughly estimate that the virial mass-to-light ratio for the region within the arc, including observational and theoretical uncertainties, is $(M/L)_R = 96 \pm 10 \pm 25$. Comparing this with the $(M/L)_R$ ratio inferred from the arc using eq. (2.2) and assuming $F < 0.2$, we find $-0.5 < \alpha < 1.9$. (We note that the M/L ratio inferred from the arc is consistent with that estimated from the smaller arclets.) This is comparable to the bound we obtained from the intracluster gas distribution, but it extends to smaller scales.

A summary of the approximate bounds on α ($|\alpha|$) for an attractive (repulsive) force as a function of the range λ is shown in fig. 1 (2). In this context, we note the recent preprint by Kawasaki, *et al.* proposing that a long-range force could allow neutrinos of mass 10 eV to cluster in dwarf galaxies, contrary to the usual phase space constraints (see the Introduction for discussion of these constraints). In particular, their required value of $\alpha \sim 10^4$ with $\lambda \gtrsim 100$ kpc is strongly ruled out by our results.

3. Cosmology and Large-Scale Structure

3.1 FRIEDMANN-ROBERTSON-WALKER MODELS

Armed with the observational constraints on a long-range force, we now turn to cosmology, the final arena where the effects of an additional dark matter interaction would be played out. First consider the evolution of a homogeneous and isotropic Friedmann-Robertson-Walker (FRW) universe; despite the form of eq. (1.4), the gravitational constant G_N is *not* replaced by a function of α in the Einstein equations. This is most easily seen by considering the scalar field example of eq. (1.1). The homogeneous field $\phi = \phi(t)$ leads to two effects: a cosmological density of coherent scalar particles, $\rho_\phi(t)$, which behaves like non-relativistic matter, and a time-dependent mass for the dark fermions. For $f \lesssim m_{pl}$ and temperatures $T \lesssim m_\phi$, both effects have negligible impact on the density of the universe. For vector fields, the situation is similar. (There are scenarios where the scalar energy density can play an important cosmological role (Frieman, Hill, and Watkins 1991), but we do not consider them here. For the cosmological implications of *massless* Brans-Dicke scalars in this context, see Damour, *et al.* (1990).) Consequently, we can assume that *the standard FRW cosmology is essentially unaltered by the additional interaction.*

This is easily verified by a simple Newtonian argument. In the Newtonian limit, which holds for non-relativistic matter and for length scales much smaller than the Hubble radius, the Robertson-Walker scale factor $a(t)$ obeys

$$3\frac{\ddot{a}}{a} = -\nabla^2\phi_g \quad (3.1)$$

where the gravitational potential ϕ_g satisfies the Poisson equation,

$$\nabla^2\phi_g = 4\pi G_N\rho. \quad (3.2)$$

Here ρ is the spatially averaged density, $\rho(t)$, and the spatial derivative is taken with respect to physical coordinates. If the universe contained only non-baryonic dark matter with an additional interaction, one might naively expect eq.(3.1) to be modified to

$$3\frac{\ddot{a}}{a} = -\nabla^2\phi_g - \nabla^2\phi_a, \quad (3.3)$$

where the potential ϕ_a for the long-range force satisfies

$$\nabla^2\phi_a - m_{v,s}^2\phi_a = 4\pi G_N\alpha\rho, \quad (3.4)$$

and $m_{v,s}$ is the mass of the exchanged vector or scalar field. However, for any non-zero mass $m_{v,s}$, eq.(3.4) has the instantaneous, spatially homogeneous solution $\phi_a^{(h)} =$

$-4\pi G_N \alpha \rho / m_{\nu, s}^2$, (this will be the approximate solution when time dependence is included as well). For this solution, $\nabla^2 \phi_a^{(h)}$ vanishes, so the additional force makes no contribution to the expansion rate of a homogeneous, isotropic cosmological model. That this must be so also follows from a two-component model containing, say, baryons and non-baryonic matter: in this case, eqs. (3.1) and (3.3) must both hold, otherwise homogeneity and isotropy would not be maintained. Since the new interaction does not violate homogeneity and isotropy, the additional potential must satisfy the homogeneous solution above.

The new force will, however, affect the growth of spatial inhomogeneities, as we shall see below.

3.2 LARGE-SCALE STRUCTURE: BACKGROUND AND SUMMARY

The observations of large-scale bulk motion (Dressler, *et al.* 1987), the sheetlike and filamentary structure seen in recent redshift surveys (*e.g.*, Geller and Huchra 1989), and the results of the deep pencil-beam surveys (Broadhurst *et al.* 1990) provide tantalizing hints of structure on large scales. Recent measurements of the galaxy angular correlation function (Maddox, *et al.* 1990, Picard 1991), the variance in galaxy counts-in-cells (Saunders, *et al.* 1991), and the correlations of rich clusters by a number of groups are beginning to provide statistical evidence for this structure.

Cold dark matter (CDM) with $\Omega = 1$ and an initial Harrison-Zel'dovich spectrum of adiabatic perturbations from inflation, long considered an attractive scenario for galaxy formation, appears to fall short in explaining at least some of these observations: there is a growing consensus that CDM produces too little power on large scales. There are different ways this difficulty might be overcome. The first possibility is to modify the primordial fluctuation spectrum. While 'designing' an arbitrary perturbation spectrum generally involves fine-tuning the potential of the field responsible for inflation, there are inflation models which naturally have at least modest amounts of additional large-scale power (Freese, Frieman, and Olinto 1990; Adams, Bond, Freese, Frieman, and Olinto 1991, in preparation); in this case, however, one must come close to saturating current microwave anisotropy limits in order to adequately account for the additional structure required. The second possibility is to modify the transfer function which determines the relative power on different scales today in terms of the initial spectrum. In this vein, possibilities include introducing a small cosmological constant (*e.g.*, Efstathiou, Sutherland, and Maddox 1990), a decaying 17 keV neutrino (Bond and Efstathiou 1991), or considering the effects of radiation pressure (Zurek 1991), the latter which, *e.g.*, may lead to a destructive interference between baryonic and dark matter perturbations on galactic scales and therefore to less power on small scales. When the spectrum amplitude is normalized in the standard way

(*e.g.*, by the second moment of the mass correlation function, J_3 , or the variance of the density field), this yields the needed excess power on *large* scales.

We show in this section that an additional long-range force may have a similar effect on the transfer function for density fluctuations. Qualitatively this is easily understood: on large scales, beyond the range of the additional interaction, the gravitational growth of perturbations is unaffected by the force. On *small* scales, however, a repulsive (attractive) force leads to reduced (enhanced) perturbation growth. If we normalize the present spectrum in the standard way, we recover more (less) relative power on *large* scales. In fact, a repulsive force of range $\lambda \gtrsim 100$ kpc and strength $\alpha \gtrsim -0.5$, consistent with the astrophysical constraints found above, can provide the additional large-scale power needed to revive the CDM scenario (with adiabatic, scale-invariant initial perturbations), without violating microwave anisotropy constraints. In addition, a repulsive force generates a bias between baryonic and dark matter perturbations on *small* scales and therefore might help explain the abundance of high-redshift quasars, despite the somewhat reduced amplitude of small wavelength perturbations. On the other hand, our analysis shows that the problems of the CDM model in accounting for large-scale structure are exacerbated by an *attractive* long-range force.

In the following we study structure formation with an additional long-range force, primarily in the context of cold-dark-matter models. In the next section we evaluate the transfer function, which describes the growth of perturbations on different scales, calculate the present fluctuation spectrum and matter correlation function, and discuss small-scale biasing. In section 3.4, we discuss the gravitationally induced large-scale streaming velocities and compare with analyses of velocity flows for different galaxy samples. In section 3.5 we study the induced anisotropies in the cosmic microwave background radiation (CMBR). In section 3.6, we discuss the relaxation of non-baryonic halos due to baryonic infall and the consequences for the disk-halo conspiracy.

3.3 PERTURBATION GROWTH AND THE POWER SPECTRUM

We assume the matter content of the Universe can be described in terms of two pressureless, ideal fluids, baryons and cold non-baryonic dark matter. As we are interested in small-amplitude perturbations inside the horizon, we can apply linear perturbation theory in the Newtonian approximation (*e.g.*, Peebles 1980; Zel'dovich and Novikov 1983). Define the fractional perturbations in the baryonic and non-baryonic matter densities by

$$\delta(\mathbf{x}, t) = \frac{\rho_b(\mathbf{x}, t) - \bar{\rho}_b(t)}{\bar{\rho}_b(t)}, \quad \Delta(\mathbf{x}, t) = \frac{\rho_{nb}(\mathbf{x}, t) - \bar{\rho}_{nb}(t)}{\bar{\rho}_{nb}(t)} \quad (3.5)$$

where $\bar{\rho}_b(t)$ and $\bar{\rho}_{nb}(t)$ are the mean baryonic and non-baryonic energy densities. Baryons are subject only to gravity, whereas the non-baryonic dark matter is also affected by the additional, nongravitational interaction. Expanding the continuity and fluid equations to first order results in

$$\begin{aligned}\bar{\delta} + 2 \left(\frac{\dot{a}}{a} \right) \dot{\delta} &= \frac{1}{a^2} \nabla_x^2 \phi_g, \\ \bar{\Delta} + 2 \left(\frac{\dot{a}}{a} \right) \dot{\Delta} &= \frac{1}{a^2} \nabla_x^2 (\phi_g + \phi_a),\end{aligned}\tag{3.6}$$

where the gradient is taken with respect to the comoving coordinate \mathbf{x} and $a(t)$ is again the cosmic scale factor. The gravitational potential, ϕ_g , satisfies the usual Poisson equation,

$$\nabla_x^2 \phi_g = 4\pi G_N a^2 (\bar{\rho}_b \delta + \bar{\rho}_{nb} \Delta).\tag{3.7}$$

The potential associated with the additional force, ϕ_a , originates solely in the dark matter perturbation and satisfies (compare eqs.(1.2) and (3.4))

$$\nabla_x^2 \phi_a - a^2 m_{v,s}^2 \phi_a = 4\pi\alpha G_N a^2 \bar{\rho}_{nb} \Delta.\tag{3.8}$$

We focus on a spatially flat, matter-dominated universe with zero cosmological constant, $\Omega = \Omega_b + \Omega_{nb} = 1$. Combining eqs. (3.6) – (3.8) and transforming to Fourier space, the evolution equations for the density fluctuations become

$$\begin{aligned}\bar{\delta}_k + \frac{4}{3t} \dot{\delta}_k - \frac{2}{3t^2} \left[\Omega_b \delta_k + \Omega_{nb} \Delta_k \right] &= 0, \\ \bar{\Delta}_k + \frac{4}{3t} \dot{\Delta}_k - \frac{2}{3t^2} \left[\Omega_b \delta_k + \left(1 + \frac{\alpha}{1 + (m_{v,s}/k_p)^2} \right) \Omega_{nb} \Delta_k \right] &= 0,\end{aligned}\tag{3.9}$$

where $k_p = k/a$ and k are the physical and comoving wavenumbers of the perturbation. (We note that the baryon pressure gradient term can easily be included in eq.(3.9).) On scales larger than the Compton wavelength of the scalar/vector particle, $k_p \ll m_{v,s}$, we retrieve the standard result for the growth of fluctuations in a flat universe, $\Delta_k = \delta_k \propto t^{2/3}$ (for the growing mode). The additional long-range force manifests itself only on small scales: in the limit $k_p \gg m_{v,s}$, the growth rate is modified to

$$\Delta_k = \frac{\delta_k}{B} \propto t^p,\tag{3.10}$$

where the ‘‘bias’’ factor B and the exponent p are given by

$$B = \frac{1}{2} \left\{ 1 - \frac{\Omega_{nb}}{\Omega_b} (1 + \alpha) + \left[\left(1 - \frac{\Omega_{nb}}{\Omega_b} (1 + \alpha) \right)^2 + 4 \frac{\Omega_{nb}}{\Omega_b} \right]^{1/2} \right\},\tag{3.11}$$

$$p = -\frac{1}{6} \left\{ 1 \pm [1 + 24(B\Omega_b + (1 + \alpha)\Omega_{nb})]^{1/2} \right\}. \quad (3.12)$$

This result merits two comments. First, although only non-baryonic matter couples to the additional interaction, the growth rate of the baryonic fluctuations is equally affected. If the baryonic mass density is small, $\Omega_b \ll (1 + \alpha)\Omega_{nb}/B$, and we have $\Omega_{nb} \simeq 1$, the power law exponent p is approximately

$$p \simeq -\frac{1}{6} \left\{ 1 \pm (25 + 24\alpha)^{1/2} \right\} \quad (3.13)$$

for scales with $k_p \gg m_{v,s}$. For an attractive force, $\alpha > 0$, the growing mode is amplified, $p > 2/3$; for example, for $\alpha = 1$, we have $p \simeq 1$ for the growing mode. For a repulsive interaction, $p < 2/3$, and the growth rate is retarded; in particular, as $\alpha \rightarrow -1$, the repulsive force completely neutralizes gravity, and $p \rightarrow 0$. The reduction in growth rate is similar to that which occurs for a matter-dominated, flat universe with two matter components, one of which is smoothly distributed and does not cluster (*e.g.*, Kolb and Turner 1990).

Second, in the small wavelength limit, the amplitudes of the baryonic and non-baryonic perturbations differ: this is manifest through the bias factor, $B(\alpha, \Omega_{nb}/\Omega_b) = \delta_k/\Delta_k$, which is larger (smaller) than unity for a repulsive (attractive) force. For a repulsive interaction, small wavelength baryonic perturbations are enhanced relative to their non-baryonic counterparts, leading to a scale-dependent bias between the dark matter and the light. An attractive force has the opposite effect and leads to anti-biasing. The fact that $B \neq 1$ for adiabatic perturbations is a direct consequence of the violation of the Equivalence principle. In fig. 3 we plot the bias factor B as a function of the force strength α , for various values of the ratio Ω_{nb}/Ω_b .

In deriving an approximate transfer function $T(k) = \Delta_k(t_0)/\Delta_k(t_i)$, which relates the perturbation amplitude today (t_0) to the amplitude when it was formed (t_i), we make the following approximations: i) We neglect the baryon density, *i.e.*, we set $\Omega_{nb} \simeq 1$ and use the approximate growth rate of eq. (3.13). ii) At early times, the physical wavelength of a given mode is smaller than the force range, $k_p^{-1} \ll m_{v,s}^{-1}$, but at late times may be conformally stretched above it. We treat this transition as discontinuous, *i.e.*, we use eq. (3.13) until $k_p^{-1} = m_{v,s}^{-1}$ and the usual growth law thereafter. iii) We neglect the small logarithmic growth of adiabatic perturbations during the radiation dominated era. To reduce the sensitivity of our results to these approximations, we also apply the last one to standard CDM perturbations and normalize the computed $T(k)$ to the fitted CDM transfer

function of Davis *et al.* (1985),

$$T^{\text{CDM}}(k) = A/(1 + \epsilon k + \omega k^{1.5} + \gamma k^2), \quad (3.14)$$

where $\epsilon = 1.7 \text{ h}^{-2} \text{Mpc}$, $\omega = 9.0 \text{ h}^{-3} \text{Mpc}^{1.5}$ and $\gamma = 1.0 \text{ h}^{-4} \text{Mpc}^2$. That is, we define the present fluctuation amplitude by

$$\Delta_k(t_0) = T^{\text{CDM}}(k) \Delta_k(t_i) \left[\frac{\Delta_k(t_0)}{\delta_k^{\text{CDM}}(t_0)} \right]_{\text{approx}} \equiv \delta_k^{\text{CDM}}(t_0) F(k), \quad (3.15)$$

where $F(k) = [\Delta_k(t_0)/\delta_k^{\text{CDM}}(t_0)]_{\text{approx}}$ denotes the modification factor with respect to standard CDM fluctuations. We calculate $F(k)$ using the three approximations above; the result is shown schematically in fig. 4. According to the second approximation, a perturbation of comoving wavenumber k is subjected to the additional long-range force until time $a_{\text{crit}} = k/m$. Furthermore, a perturbation crosses inside the horizon (in a matter dominated universe) at $a_{\text{hor}}(k) = (2\pi/ct_0)^2 k^{-2} \simeq 2.47 \times 10^{-6} k^{-2}$ (k is given in Mpc^{-1}). The characteristic wavenumbers in fig. 4 are then defined by $a_{\text{hor}}(k_{\text{eq}}) = a_{\text{eq}}$, $a_{\text{hor}}(k_n) = a_{\text{crit}}(k_n)$ and $a_{\text{crit}}(k_a) = a_0 = 1$, where a_{eq} is the scale factor at equal matter and radiation energy densities. (For our choices of $m_{\nu,s}$, $k_n < k_{\text{eq}} < k_a$.) Perturbations with $k > k_a$ never stretched beyond the force range and were therefore always subjected to the additional interaction. In contrast, fluctuations with $k < k_n$ were already outside the range at horizon crossing and thus always experienced standard gravity.

The initial spectrum of perturbations $\Delta_k(t_i)$ is taken to be scale-invariant, $|\Delta_k(t_i)|^2 \propto k$. We normalize the power spectrum by the second moment of the mass correlation function, evaluated from the CfA red-shift survey (Davis and Peebles 1983), $J_3(10h^{-1}\text{Mpc}) = 270 \text{ h}^{-3} \text{Mpc}^3$, where

$$J_3(r) = \frac{V}{2\pi^2} \int_0^\infty |\Delta_k(t_0)|^2 (\sin kr - kr \cos kr) \frac{dk}{k}. \quad (3.16)$$

(Normalizing by the variance of the density field at $8h^{-1}\text{Mpc}$ with a top-hat window function yields a similar result.) Note that in choosing this normalization, we have implicitly made two assumptions: (i) that the characteristic normalization scale, $r \sim 8h^{-1} \text{Mpc}$, is large compared to the Compton wavelength λ so that the bias factor $B(\alpha)$ does not enter the normalization ($B(\alpha, 8h^{-1}\text{Mpc}) = 1$) (however, see the discussion at the end of this subsection); (ii) that there are no other sources of bias in linear perturbation theory.

Fig. 5 shows the processed power spectrum for different values of the force strength α and force range λ . (In our numerical calculations we assume the Hubble parameter is $H_0 = 50 \text{ km sec}^{-1} \text{ Mpc}^{-1}$, i.e., $h=1/2$.) In the long-wavelength limit, where the additional interaction is inoperative, the spectra exhibit identical slopes, and differ only in overall amplitude due to the normalization on small scales. On small scales, however, an extra force generates distinctive features in the fluctuation spectrum. The deviation from the standard CDM result becomes evident with increasing force range and/or enhanced strength. As noted above, an attractive force diminishes the power at long wavelengths and is therefore less successful than standard CDM in explaining structure formation on large scales. On the other hand, a repulsive interaction reduces the amplitude of small wavelength perturbations and therefore relatively enhances the power on large scales.

The magnitude of this effect becomes more transparent by studying the spatial two-point mass correlation function,

$$\xi(r) = \frac{V}{2\pi^2} \int_0^\infty |\Delta_k(t_0)|^2 \frac{\sin kr}{kr} k^2 dk. \quad (3.17)$$

In fig. 6 we plot $\xi(r)$ for $\alpha = -0.3$ and -0.5 for several values of the force range λ . Here the short-dash-dotted line shows the standard power law fit to the data on scales $r \lesssim 10h^{-1} \text{ Mpc}$, $\xi(r) = (r/5.6h^{-1} \text{ Mpc})^{-1.8}$, and the solid curve presents the standard CDM result ($\alpha = 0$). Since this is a linear perturbation theory calculation, it is only to be trusted on scales larger than $r \sim 20 \text{ Mpc}$ (for $h = 0.5$); the key point is that models with even a modest repulsive force can have substantial excess large-scale power.

To compare with observations, in fig. 7 we show the angular two-point correlation function $w(\theta)$ for models with a repulsive force, $\alpha = -0.3$ and the same values of λ as above. The angular two-point function was calculated from $\xi(r)$ (here normalized to $\xi(4.6h^{-1} \text{ Mpc}) = 1$) using the relativistic form of Limber's equation (see, e.g., Peebles 1980) assuming $\Omega = 1$, with the Schechter luminosity function of Maddox, *et al.* (1990); the observer selection function was assumed to be unity over the apparent magnitude interval $17 < b_J < 20$, corresponding to the depth of the APM galaxy survey. For comparison we show the data from the APM galaxy survey (Maddox, *et al.* 1990) and the POSS-II survey (Picard 1991), which has nearly identical depth. (Note that the data has *not* been rescaled in depth.) The standard cold dark matter model (solid curve) falls short of the APM data on large angular scales (Maddox, *et al.* 1990), while a CDM model with a repulsive force of strength $\alpha = -0.3$ and range $\lambda = 100 \text{ kpc}$ fits the data out to 5° remarkably well.

Throughout this discussion, we have been assuming that the Compton wavelength of the additional interaction is short compared to the characteristic normalization scale for large-scale structure, $\lambda \lesssim 8h^{-1}$ Mpc. As a final comment, we note here the results for the opposite case of a very-long-range force, $\lambda \gtrsim 1000h^{-1}$ Mpc. In this case, perturbations on all observable length scales are equally affected by the additional force, so that, aside from a change in overall normalization, the perturbation transfer function $T(k)$ is just that for cold dark matter, eq.(3.14). That is, the modification factor $F(k)$ entering eq.(3.15) is k -independent; the only change from standard (unbiased) CDM is that the Δ spectrum should be normalized by setting $J_3(10h^{-1}\text{Mpc}) = B^{-2}(\alpha) 270h^{-3} \text{Mpc}^3$, where the bias factor $B(\alpha)$ is given by eq.(3.11) (Fig. 3). The implications for microwave anisotropy constraints will be discussed below.

3.4 LARGE-SCALE VELOCITY FIELD

One of the major drawbacks of the standard CDM scenario lies in its apparent difficulty in reproducing the observed peculiar velocity field on large scales. Here we study how an additional long-range force affects this problem. As we would expect from the preceding section, models with a repulsive force lead to additional large-scale power and can help cure this difficulty.

From the continuity equation, we can evaluate the gravitationally induced (linear) comoving peculiar velocity (Peebles 1980; Zel'dovich and Novikov 1983)

$$\mathbf{u}_k(t) = -i\frac{\mathbf{k}}{k^2} \dot{\Delta}_k(t) = -i\frac{\mathbf{k}}{k^2} H_0 \Delta_k(t_0) f(k, t_0), \quad (3.18)$$

where the function $f = d(\ln D)/d(\ln a)$, and $D(t, k)$ describes the time-evolution of the fluctuation amplitude, $\Delta_k(t) = D(t, k)\Delta_k(t_0)$. In contrast to the standard ($\alpha = 0$) scenario, f is now k -dependent: $f(k, t_0) = 1$ ($3p/2$) for $k \ll m_{v,s}$ ($k \gg m_{v,s}$), where p is the power law exponent given by eq. (3.12) or (3.13), and we have set $a_0 = 1$. Note that α does not appear explicitly in eq. (3.18), but only indirectly through its modification of the growth rate p . From (3.18) we can estimate the expected mean square bulk velocity of a spherical volume of radius r (Clutton-Brock and Peebles 1981; Kaiser 1983),

$$v_{\text{rms}}^2(r) = \frac{H_0^2}{2\pi^2} \int_0^\infty f^2(k, t_0) |\Delta_k(t_0)|^2 W_g^2(kr) dk, \quad (3.19)$$

where $W_g(kr)$ is a window function.

Fig. 8 shows the rms bulk velocity, eq. (3.19), calculated with a Gaussian window function, $W_g(kr) = \exp(-k^2r^2/2)$, using the same values of λ as before. We also plot two fitted data points with their estimated error bars. The higher velocity of 600 ± 100 km/sec on a scale of $60 h^{-1}\text{Mpc}$ (120 Mpc with $h=1/2$) was obtained from a sample of nearby elliptical galaxies by Dressler *et al.* (1987). The lower bulk velocity, 570 ± 60 km/sec, of a volume of size $43.5 h^{-1}\text{Mpc}$, corresponds to the fitted value in the ‘‘Great Attractor’’ model (Lynden-Bell *et al.* 1988). The standard CDM model, shown by the solid curves, predicts velocities of order 200 km/sec on these scales. A repulsive force does considerably better than standard CDM in generating the large-scale streaming velocity: a scenario with $\alpha \simeq -0.5$ and $1 \text{ Mpc} \lesssim \lambda \lesssim 10 \text{ Mpc}$ is consistent with the observational data. (Note that a force of strength $\alpha = -0.3$ still falls short in explaining the observations.) At the same time, an *attractive* force of range $\lambda \gtrsim 10 \text{ kpc}$ exacerbates the velocity problem, and is essentially excluded in the context of the CDM scenario with adiabatic, scale-invariant primordial fluctuations.

Based on a potential flow reconstruction algorithm (Bertschinger and Dekel 1989; Dekel, Bertschinger and Faber 1990), Bertschinger *et al.* (1990) have recently constructed maps of the large-scale velocity and density field from redshift-distance samples. Their selection function for the bulk flow estimates on a given scale r is a convolution of a top-hat window function, $W_{th} = 3[\sin(kr) - kr \cos(kr)]/(kr)^3$, with a Gaussian filter of radius $r_s = 12 h^{-1}\text{Mpc}$, $W_{sm} = \exp(-k^2r_s^2/2)$. The additional Gaussian smooths the data on small scales. The expected large-scale streaming velocity is then defined by

$$u(r)^2 = \frac{H_0^2}{2\pi^2} \int_0^\infty f^2(k, t_0) |\Delta_k(t_0)|^2 W_{th}^2(kr) W_{sm}^2(kr_s) dk . \quad (3.20)$$

From the reconstructed three-dimensional velocity field, Bertschinger *et al.* (1990) estimate average streaming velocities $u(r) = 388 \pm 67$ km/sec and 327 ± 82 km/sec in spheres of radii $40 h^{-1}\text{Mpc}$ and $60 h^{-1}\text{Mpc}$. The expected velocities in the standard CDM model are only $\sim 30\%$ below these values. Fig. 9 shows the bulk velocity $u(r)$ for various model parameters α and λ . A repulsive force of strength $\alpha \simeq -0.5$ and range $1 \text{ Mpc} \lesssim \lambda \lesssim 10 \text{ Mpc}$, although consistent with the rms bulk flow $v_{rms}(r)$ estimated by Dressler *et al.* (1987) as seen above, produces streaming velocities $u(r)$, according to eq. (3.20), well in excess of the observations. For consistency with the data on $u(r)$, we must either limit the range of the additional interaction to $\lambda \simeq 10 \text{ kpc}$ or reduce its strength to $\alpha = -0.3$ (with range $100 \text{ kpc} \lesssim \lambda \lesssim 10 \text{ Mpc}$).

An alternative, normalization-independent test of the power spectrum using velocity data is the Cosmic Mach number, $\mathcal{M}(r)$ (Ostriker and Suto 1990). The Mach number

characterizes the ratio of the coherent bulk velocity of an ensemble of objects to the internal velocity dispersion of the objects,

$$\mathcal{M}(r) = \left\{ \frac{\int_0^\infty |\Delta_{\mathbf{k}}(t_0)|^2 W_g^2(kr) W_{\text{sm}}^2(k\xi) dk}{\int_0^\infty |\Delta_{\mathbf{k}}(t_0)|^2 \left[1 - \left(1 + \frac{k^2 r^2}{9}\right) W_g^2(kr) \right] W_{\text{sm}}^2(k\xi) dk} \right\}^{1/2}, \quad (3.21)$$

where we have again smoothed the velocity field by an additional Gaussian window function, $W_{\text{sm}}(k\xi)$; Ostriker and Suto (1990) consider a smoothing length $\xi = 5 h^{-1} \text{Mpc}$. From the peculiar velocity samples, they extract $\mathcal{M}(16 \pm 3.6 \text{ Mpc}) = 2.2 \pm 0.5$ for spiral galaxies and $\mathcal{M}(36 \pm 7.0 \text{ Mpc}) = 1.3 \pm 0.4$ for ellipticals (Ostriker and Suto 1990). Fig. 10 shows the expected Mach number for various values of α and λ within the context of CDM. The standard CDM model with $\alpha = 0$ again appears to be incompatible with the observations, due to the shortage of power on large scales. A scenario with an *attractive* force is even less successful than standard CDM, while a repulsive force can increase the Mach number of the CDM model to be compatible with the observed values.

By inspection of figs. 8 – 10 it appears that the large-scale bulk flow found by Dressler *et al.* (1987), the average streaming velocity from the redshift-distance samples (Bertschinger *et al.* 1990), and the Cosmic Mach number results (Ostriker and Suto 1990) are mutually incompatible. Coupled with the CDM model, a relatively weak and/or ‘short range’ repulsive force can reproduce the average velocities found by Bertschinger *et al.*, while a stronger interaction of long range is required to obtain the high velocities reported by Dressler *et al.*

3.5 ANISOTROPY OF THE MICROWAVE BACKGROUND RADIATION

The angular isotropy of the CMBR provides one of the most sensitive constraints on fluctuation spectra. We focus on large-scale, sub-horizon scale irregularities in the background temperature due to the Sachs-Wolfe effect (Sachs and Wolfe 1967; Peebles 1980), which dominates on angular scales larger than a few degrees. After an integration by parts, the temperature fluctuation can be written as

$$\Delta T/T = \Sigma + \Xi. \quad (3.22)$$

Here, Σ is the familiar boundary term due to the gravitational potential Φ at the last-

scattering surface,

$$\Sigma = -\frac{3}{2} p_0 \left(p_0 - \frac{1}{3} \right) \Phi(\mathbf{x} = \mathbf{x}_0), \quad (3.23)$$

while Ξ includes an integration along the line of sight (Peebles 1980; for a recent discussion, see *e.g.*, Sahni, *et al.* 1991),

$$\Xi = \int_{t_{dec}}^{t_0} \nabla^{-2} \Delta(t_0, \mathbf{x}(t)) \Gamma(t) dt, \quad (3.24)$$

where

$$\mathbf{x}(t) = \mathbf{x}_0 + \hat{\mathbf{n}} \int_t^{t_0} \frac{dt}{a}, \quad \Gamma(t) = \frac{d}{dt} a \frac{d}{dt} a \frac{d}{dt} D(t). \quad (3.25)$$

Here, $p_0 \equiv p(k, t_0)$ is the power law exponent given by eq. (3.12) or (3.13), $\hat{\mathbf{n}}$ is the direction vector along the line of sight, and t_{dec} is the cosmic time at the epoch of last scattering. In the case of standard (linear) CDM fluctuations in a spatially flat universe, the fluctuation growth rate $D(t) \propto a(t)$, so that the line of sight term $\Xi \equiv 0$, and the Σ -term reduces to the familiar result, $\Sigma = -\frac{1}{3} \Phi(\mathbf{x} = \mathbf{x}_0)$.

If, however, $D(t) \not\propto a(t)$, then the gravitational potential associated with growing mode perturbations is time-dependent; as a result, the line-of-sight term due to the photon blue- and redshift as it falls into and climbs out of a developing potential well does not cancel out. The expected mean square anisotropy in any direction is then given by

$$\langle (\Delta T/T)_\alpha^2 \rangle = \langle |\Sigma|^2 \rangle + \langle |\Xi|^2 \rangle + 2 \langle |\Sigma \Xi| \rangle, \quad (3.26)$$

where

$$\langle |\Sigma|^2 \rangle = \frac{81}{32\pi^2} H_0^4 \int_0^\infty dk p_0^2 \left(p_0 - \frac{1}{3} \right)^2 \frac{|\Delta_k(t_0)|^2}{k^2}, \quad (3.27)$$

$$\begin{aligned} \langle |\Xi|^2 \rangle &= \frac{1}{2\pi^2} \int_0^\infty dk \int_{t_{dec}}^{t_0} dt_1 \int_{t_{dec}}^{t_0} dt_2 \Gamma(t_1) \Gamma(t_2) \\ &\quad \times \frac{\sin k|\mathbf{x}(t_1) - \mathbf{x}(t_2)|}{k|\mathbf{x}(t_1) - \mathbf{x}(t_2)|} \frac{|\Delta_k(t_0)|^2}{k^2}, \end{aligned} \quad (3.28)$$

$$\begin{aligned}
\langle |\Sigma \Xi| \rangle &= -\frac{9}{8\pi^2} H_0^2 \int_0^\infty dk \int_{t_{dec}}^{t_0} dt p_0 \left(p_0 - \frac{1}{3} \right) \Gamma(t) \\
&\quad \times \frac{\sin k|\mathbf{x}(t) - \mathbf{x}_0|}{k|\mathbf{x}(t) - \mathbf{x}_0|} \frac{|\Delta_k(t_0)|^2}{k^2}.
\end{aligned} \tag{3.29}$$

We have numerically evaluated the three terms of eq. (3.26) and find that, except in the extreme case of a strong and very long-range repulsive force, $\alpha \lesssim -0.8$ and $\lambda \gtrsim 1$ Mpc, which is ruled out by the considerations of Section II, the last two terms are subdominant and can be neglected to first approximation; hence $(\Delta T/T)_\alpha \simeq (|\Sigma|^2)^{1/2}$.

To compare with the observational constraints, we calculate the temperature autocorrelation function on angular scale θ

$$\begin{aligned}
C(\theta) &= \left\langle \frac{\Delta T(\hat{n}_1)}{T} \frac{\Delta T(\hat{n}_2)}{T} \right\rangle \\
&= \frac{81}{32\pi^2} H_0^4 \int_0^\infty dk p_0^2 \left(p_0 - \frac{1}{3} \right)^2 \frac{|\Delta_k(t_0)|^2}{k^2} \\
&\quad \times \left[j_0(ky) - j_0^2(kR_H) - 3 \cos \theta j_1^2(kR_H) \right],
\end{aligned} \tag{3.30}$$

where j_n are spherical Bessel functions, $R_H = 2/H_0$ is the present horizon scale, $\hat{n}_1 \cdot \hat{n}_2 = \cos \theta$, and $y = 2R_H \sin(\theta/2)$. In eq. (3.30) we have subtracted the monopole and dipole terms from the total autocorrelation function (Peebles 1982; Martínez-González and Sanz 1989; Górski 1991). The monopole component corresponds to a small change in the mean temperature and is unobservable from a single location. The dipole moment is attributed to the peculiar motion of the Local group with respect to the comoving frame; it dominates the higher moments of the CMBR anisotropy and is usually subtracted from the observational data.

We can compare the theoretical temperature correlation function $C(\theta)$ from eq. (3.30) with the observational limits from the COBE satellite (Smoot *et al.* 1991),

$$C(\theta) < 1.0 \cdot 10^{-9}, \quad \text{for } 15^\circ < \theta < 165^\circ. \tag{3.31}$$

In fig. 11 we plot our results for various sets of parameters α and λ . The shaded area represents the region excluded by the COBE results. Aside from the model with a repulsive force of strength $\alpha = -0.5$ and range $\lambda \gtrsim 10$ Mpc, the CDM scenarios with an additional force are clearly consistent with the measurements.

We can also evaluate the quadrupole moment of the CMBR anisotropy and compare it to the observational limits from the RELIKT experiment (Strukov *et al.* 1987) and COBE (Smoot *et al.* 1991). Both groups place the bound $C_2^{1/2} < 3.0 \cdot 10^{-5}$ at the 95 % confidence level. The temperature autocorrelation function can be expressed as a multipole expansion, normalized to the quadrupole moment of the CMBR anisotropy. For scale-invariant fluctuations, one can then find the quadrupole moment from (Efstathiou 1990)

$$C(\theta) = \frac{3}{2\pi} C_2 \left[\ln \left(\frac{2}{1 - \cos \theta} \right) - 1 - \frac{3}{2} \cos \theta \right], \quad (3.32)$$

with $\theta \gg 1^\circ$. In models with a repulsive force, $C(\theta)$ is dominated by the long wavelength regime, where the shape of the power spectrum coincides with the standard CDM spectrum. In this case, the anisotropy is mainly affected by the change in small-scale normalization and is therefore expected to have the same θ -dependence as in eq. (3.32). For attractive interactions, however, the temperature autocorrelation function is also influenced by the large fluctuation power on *small* wavelengths, where the shape of the power spectrum deviates significantly from the standard CDM result. In this case, we cannot rely, *a priori*, on the relation (3.32), but must evaluate the quadrupole moment explicitly,

$$C_2 = \frac{81}{8\pi} H_0^4 \int_0^\infty dk p_0^2 \left(p_0 - \frac{1}{3} \right)^2 \frac{|\Delta_k(t_0)|^2}{k^2} j_2^2(kR_H). \quad (3.33)$$

In fig. 12 we plot the quadrupole moment, $C_2^{1/2}$, as a function of α for different values of the force range λ . The shaded area denotes the region excluded by the RELIKT and COBE experiments. We again note that only very long-range repulsive forces, with $\alpha \lesssim -0.4$ and $\lambda \gtrsim 10$ Mpc, are ruled out. In particular, CDM with an extra force of strength $\alpha \gtrsim -0.5$ and range $\lambda \lesssim 1$ Mpc can reproduce the large-scale velocity field and yet is consistent with both CMBR anisotropy constraints and our previously derived astrophysical bounds.

Finally, we mention the CMBR constraints on the very-long-range-force models discussed at the end of section 3.3. Recall that in this case, $\lambda \gtrsim 1000h^{-1}$ Mpc, we recover the usual CDM spectrum, modified by the overall bias factor $1/B(\alpha)$. From fig. 3 and eq. (3.23) it is clear that the amplitude of the large-scale anisotropy will be altered from the standard unbiased CDM prediction. In particular, the *rms* Sachs-Wolfe anisotropy is given by

$$\frac{\Delta T}{T}(\alpha) = \frac{\Delta T}{T}(0) \frac{9}{2} p(\alpha) \left(p(\alpha) - \frac{1}{3} \right) B^{-1}(\alpha) \quad (3.34)$$

where $B(\alpha)$ and $p(\alpha)$ are given by eqs.(3.11) and (3.12). For example, for an attractive

force with strength $\alpha = 1$, the anisotropy is increased by a factor of about 5.8 compared to standard, unbiased CDM; this is in conflict with the COBE and RELIKT bounds. Requiring the enhancement factor on the RHS of eq. (3.34) to be less than 3, we find the CMBR constraint $\alpha \lesssim 0.6$ for a very long-range attractive force.

It is worth repeating that our analysis of structure formation has been carried out exclusively in the framework of a CDM-dominated universe with adiabatic, scale-invariant primordial perturbations. An extra force may have significantly different effects in other scenarios for large-scale structure formation.

3.6 HALO RESPONSE AND NON-LINEAR CLUSTERING

A final bound on the force strength α results from considering the response of dark halos to dissipational baryonic infall in the non-linear stages of galaxy formation. For a collisionless dark matter particle in a circular orbit in a protogalaxy, conservation of angular momentum implies a relation between its initial radius r_i (before baryonic infall) and its final radius r , after the baryons have cooled and collapsed into a disk (Ryden and Gunn 1984, Blumenthal, *et al.*, 1986, Barnes 1987). We first review the argument for the standard case, $\alpha = 0$, following Blumenthal, *et al.* (1986). Let $M_i(r_i)$ be the total (baryon plus non-baryonic) protogalaxy mass interior to the initial halo particle radius r_i , $M_b(r)$ be the final dissipational baryon mass distribution in the disk, and $M_z(r)$ be the final dark matter distribution, and assume that initially there is no segregation on the protogalaxy scale, *i.e.*, the initial dissipational baryon mass fraction, $F = M_b(r_i)/M_i(r_i)$, is independent of radius. If the halo orbits do not cross, then $M_z(r) = (1 - F)M_i(r_i)$ is the final halo mass inside radius r , and the initial and final particle radii are related by

$$\frac{r_i}{r} = \frac{M_b(r) + M_z(r)}{M_i(r_i)} = f(r/l)F + 1 - F. \quad (3.35)$$

Here, the function $f(r/l)$ is determined completely by the disk scale length l and the ratio of the core radius to the outer radius of the initial mass distribution (assumed to be a truncated isothermal sphere); it is independent of F . The resulting rotation curve is found to be relatively flat and continuous from the baryon-dominated core to the dark-matter-dominated halo only if F lies in the range (Blumenthal, *et al.*, 1986) $0.05 < F < 0.2$. That is, for this range of parameters, the relaxation of the halo due to dissipational infall of the baryons can account reasonably well for the disk-halo ‘conspiracy’, namely, the fact that rotation curves do not have a prominent feature where the halo begins to dominate over the disk (Bahcall and Casertano 1985).

Repeating the above procedure allowing for $\alpha \neq 0$, the conserved quantity is now $r[(1 + \alpha)M_z(\tau) + M_b(\tau)]$. In place of eq.(3.35) we now have

$$\frac{r_i}{r} = \frac{M_b(\tau) + (1 + \alpha)M_z(\tau)}{M_i(r_i)(1 + \alpha - \alpha F)} . \quad (3.36)$$

Defining a new variable,

$$\bar{F} = \frac{F}{1 + \alpha - \alpha F} , \quad (3.37)$$

we can rewrite eq.(3.36) as

$$\frac{r_i}{r} = f(\tau/l)\bar{F} + 1 - \bar{F} . \quad (3.38)$$

Since this has the same form as eq. (3.35), the requirement of flat rotation curves now yields the constraint $0.05 < \bar{F} < 0.2$.

To translate this constraint into a bound upon α , we must introduce an additional assumption. First, if we assume that essentially all baryons cluster dissipatively with galaxies, we expect the dissipational baryon fraction to be $F = M_{b_i}/M_i \simeq \Omega_b$. From big bang nucleosynthesis, we have the conservative bounds on the baryon density $0.007 < \Omega_b < 0.21$ (*e.g.*, Kolb and Turner 1990). Using nucleosynthesis to constrain F , and the rotation curve bound on \bar{F} , we find the constraint $-1 < \alpha < 4$ for a force range comparable to the galaxy scale or larger. However, this argument does not take into account the scale-dependent bias, eq.(3.11), between the baryons and the dark matter. For a perturbation with baryon mass δM_b and nonbaryonic mass δM_{nb} , we have, on small scales,

$$\frac{\delta M_b}{\delta M_{nb}} = B \frac{\bar{\rho}_b}{\bar{\rho}_{nb}} = \frac{B \Omega_b}{1 - \Omega_b} , \quad (3.39)$$

where $B(\alpha, \Omega_b)$ is the linear bias parameter given in eq.(3.11) and we have again assumed a spatially flat universe. Thus, the expected baryon fraction in the protogalaxy perturbation is

$$F = \frac{\delta M_b}{\delta M} = \frac{B \Omega_b}{1 + \Omega_b(B - 1)} . \quad (3.40)$$

Using the nucleosynthesis constraint on Ω_b and the rotation curve bound on \bar{F} , we now find the constraint $-0.8 < \alpha < 1.3$. (Alternatively, one could constrain α as a function of Ω_b .) If α is outside this range, spiral rotation curves would be sharply rising or steeply falling instead of nearly flat. This constraint is also included in Fig. 1. (We note that, unlike the other bounds shown there, the latter constraint depends on the additional assumptions about linear clustering and CDM introduced above.)

4. Conclusion

We have touched upon only a few of the many interesting phenomena which arise if the dark matter violates the principle of equivalence in the sense of interacting with 'hidden' long-range forces. From mass-to-light ratios in galaxies and binaries, the gas distribution in clusters, luminous arcs, and the relaxation of dark halos due to baryonic infall, we conclude that the relative strength of such an interaction must satisfy $-0.5 \lesssim \alpha \lesssim 1.3$ if its range $\lambda \gtrsim$ a few hundred kpc. Even so, such an interaction can alter the apparent density of dark matter and profoundly change the spectrum and amplitude of large-scale density fluctuations.

Acknowledgements

We thank R. Flores, E. Gaztañaga N. Kaiser, J. Primack, J. Quashnock, and Y. Suto for useful conversations. Parts of this work were completed at the 1991 Aspen Center for Physics summer workshop. This work was supported in part by the DOE and by NASA grant NAGW-2381 at Fermilab.

REFERENCES

- Bahcall, J., and Casertano, S. 1985, *Ap. J. Lett.* **293**, L7.
Bahcall, J., Piran, T., and Weinberg, S., eds., *Dark Matter in the Universe*, Jerusalem Winter School for Theoretical Physics, vol. 4, (World Scientific, 1987).
Barnes, J. 1987, in *Nearly Normal Galaxies*, ed. Faber, S. M. (Springer-Verlag, 1987).
Bars, I., and Visser, M. 1986, *Phys. Rev. Lett.* **57**, 25.
Bertschinger, E. and Dekel, A. 1989, *Ap. J. (Letters)*, **336**, L5.
Bertschinger, E., Dekel, A., Faber, S.M., Dressler, A. and Burstein, D. 1990, *Ap. J.*, **364**, 370.
Binney, J., and Tremaine, S. 1987, *Galactic Dynamics* (Princeton University Press, 1987).
Blumenthal, G. R., Faber, S. M., Flores, R., and Primack, J. R. 1986, *Ap. J.* **301**, 27.
Bothun, G., and Schombert, J. 1988, *Ap. J.* **335**, 617.
Broadhurst, T.J., Ellis, R.S., Koo, D.C., and Szalay, A.S. 1990, *Nature*, **343**, 726.
Carney, B., and Latham, D. 1987, in *Dark Matter in the Universe*, IAU Symposium No. 117, ed. J. Kormendy and G. R. Knapp (Dordrecht: Reidel).
Cavaliere, A., and Fusco-Femiano, R. 1976, *Astron. Astrophys.* **49**, 137.
Cline, J., Raby, S., Scherrer, R., and Seckel, D. 1991, preprint.

- Clutton-Brock, M. and Peebles, P.J.E. 1981, *Ap. J.*, **86**, 115.
- Cudworth, K. Cudworth, K. 1990, *Astron. J.* **99**, 590.
- Damour, T., Gibbons, G. W., and Gundlach, C. 1990, *Phys. Rev. Lett.* **64**, 123.
- Davis, M., and Huchra, J. 1982, *Ap. J.* **254**, 437.
- Davis, M., and Peebles, P.J.E 1983, *Ap. J.*, **267**, 465.
- Davis, M., Efstathiou, G., Frenk, C. and White, S.D.M. 1985, *Ap.J.*, **292**, 371.
- Dekel, A., Bertschinger, E. and Faber, S.M. 1990, *Ap. J.*, **364**, 349.
- Dressler, A., Faber, S.M., Burstein, D., Davies, R.L., Lynden-Bell, D., Terlevich, R.J., and Wegner, G. 1987, *Ap. J. (Letters)*, **313**, L37.
- Efstathiou, G. 1990, University of Oxford preprint, OUAST/90/96.
- Efstathiou, G., Sutherland, W., and Maddox, S. 1990, *Nature* **348**, 705.
- Evrard, A. E. 1990, in *Clusters of Galaxies*, Space Telescope Science Institute Proceedings, eds. Oegerle, W., Fitchett, M., and Danly, L. (Cambridge University Press), p. 287.
- Fackler, O., and Tran Thanh Van, J., eds. 1989, *Tests of Fundamental Laws in Physics*, Proc. of the XXIV Rencontre de Moriond, (Editions Frontieres, Gif-sur-Yvette, France 1989).
- Fich, M., and Tremaine, S. 1991, *Ann. Rev. Astron. Astrophys.* **29**, 409.
- Fitchett, M. 1990, in *Clusters of Galaxies*, eds. Oegerle, W., Fitchett, M., and Danly, L. (Cambridge University Press), p. 111.
- Freese, K., Frieman, J., and Olinato, A. 1990, *Phys. Rev. Lett.* **65**, 3233.
- Frieman, J., and Gradwohl, B. 1991, *Phys. Rev. Lett.* **67**, 2926.
- Frieman, J., Hill, C. T., and Watkins, R. 1991, Fermilab preprint.
- Geller, M.J., and Huchra, J.P. 1989, *Science*, **246**, 897.
- Górski, K.M. 1991, *Ap. J. (Letters)*, **370**, L5.
- Hegyi, D., and Olive, K. 1986, *Ap. J.* **303**, 56.
- Henry, J. P., and Lavery, R. J. 1987, *Ap. J.* **323**, 473.
- Hill, C. T., and Ross, G. G. 1988, *Nucl. Phys.* **B311** (1988/89) 253.
- Jones, C., and Forman, W. 1984, *Ap. J.* **276**, 38.
- Kaiser, N. 1983, *Ap. J. (Letters)*, **273**, L17.
- Kirshner, R., Oemler, A., Schechter, P., and Shectman, S. 1983, *Astron. J.* **88**, 1285.
- Kolb, E.W., and Turner, M.S. 1990, *The Early Universe*, (Addison-Wesley Publishing Company 1990), p. 348.
- Lauer, T. 1988, *Ap. J.* **325**, 49.
- Leonard, P. J. T., and Tremaine, S. 1990, *Ap. J.* **353**, 486.
- Lynden-Bell, D., Faber, S.M., Burstein, D., Davies, R.L., Dressler, A., Terlevich, R.J., and Wegner, G. 1988, *Ap. J.*, **326**, 19.

- Lynds, R., and Petrosian, V. 1986, *Bull. Am. Astr. Soc.* 18, 1014.
- Maddox, S., Efstathiou, G., Sutherland, W., and Loveday, J. 1990, *Mon. Not. R. Astr. Soc.* 242, 43p.
- Martinez-González, E. and Sanz, J.L. 1989, *Ap. J.*, 347,11.
- Merritt, D. 1984, *Ap. J.* 276, 26.
- Merritt, D. 1987, *Ap. J.* 313 121.
- Mellier, Y., Soucail, G., Fort, B., and Mathez, G. 1988, *Astron. Astrophys.* 199, 13.
- Mellier, Y., *et al.*, eds. 1990, *Gravitational Lensing*, (Springer Verlag).
- Moran, J., *et al.*, eds. 1988, *Gravitational Lenses*, (Springer Verlag).
- Mushotsky, R. F. 1984, *Phys. Scripta*, T7, 157.
- Oegerle, W., Fitchett, M., and Danly, L., eds. 1990, *Clusters of Galaxies*, Space Telescope Science Institute Proceedings (Cambridge University Press).
- Ostriker, J.P., and Suto, Y. 1990, *Ap. J.*, 348, 378.
- Pakvasa, S., Simmons, W. A., and Weiler, T. J. 1989, *Phys. Rev.* D39, 1761.
- Peebles, P.J.E. 1980, *The Large-Scale Structure of the Universe*, (Princeton University Press, Princeton 1980).
- Peebles, P.J.E. 1982, *Ap. J. (Letters)*, 263, L1.
- Primack, J. R., Seckel, D., and Sadoulet, B. 1988, *Ann. Rev. Nucl. Part. Sci.* 38, 751.
- Picard, A. 1991, *Ap. J.* 368, L7.
- Pryor, C., and Geller, M. 1984, *Ap. J.* 278, 457.
- Raffelt, G., and Silk, J. 1987, *Phys. Lett.* 129, 65.
- Ryden, B. and Gunn, J. 1984, *Bull. AAS* 16, 487.
- Sachs, R.K., and Wolfe, A.M. 1967, *Ap. J.*, 147, 73.
- Sahni, V., Feldman, H., and Stebbins, A. 1991, CITA preprint.
- Sarazin, C. 1988, *X-ray Emission from Clusters of Galaxies*, (Cambridge University Press).
- Saunders, W. *et al.* 1990, *Nature* 349, 32.
- Scherk, J. 1980, in *Unification of the Fundamental Particle Interactions*, eds. Ferrara, S., Ellis, J., and van Nieuwenhuizen, P. (Plenum Press, 1980).
- Smoot, G.F. *et al.* 1991, *Ap. J. (Letters)*, 371, L1.
- Soucail, G., Fort, B., Mellier, Y., and Picat, J. P. 1987, *Astron. Astrophys.* 172, L14.
- Soucail, G., Mellier, Y., Fort, B., Mathez, G., and Cailloux, M. 1988, *Astron. Astrophys.*, 191, L19.
- Spergel, D., Gott, J. R. III, and Weinberg, D. 1988, *Phys. Rev.* D38, 2014.
- Strukov, I.A., Skulachev, D.P., and Klypin, A.A. 1987, in *Large Scale Structure of the Universe*, (IAU Symposium, edited by Audouze, J., Pelletan, M-C., and Szalay, H., (Kluwer, Dordrecht), p. 27.

- Tremaine, S. and Gunn, J. E. 1979, *Phys. Rev. Lett.* **42**, 407.
- van Albada, T. S., Bahcall, J. N., Begeman, K., and Sancisi, R. 1985, *Ap. J.* **295**, 305.
- Whitmore, B., Forbes, D., and Rubin, V. 1988, *Ap. J.* **333**, 542.
- Zel'dovich, Ya.B., and Novikov, I.D. 1983, *Relativistic Astrophysics*, vol. 2, ed. Steigman, G. (The University of Chicago Press, Chicago 1983).
- Zurek, W.H. 1991, *Ap. J.* **370**, 474.

FIGURE CAPTIONS

- 1) Astrophysical bounds on the strength α of an attractive force as a function of range λ . The limits arise from: M/L of the Local group (solid curve); rotation curves of cluster galaxies (dotted curve); intracluster gas (short-dashed curve); luminous arcs (long-dashed curve); and halo relaxation (dot-dashed curve).
- 2) Bounds on the strength $|\alpha|$ of a repulsive force as a function of range λ : gravitationally bound halos (solid curve); intracluster gas (dotted curve); luminous arcs (short-dashed curve); and halo relaxation (long-dashed curve).
- 3) Bias factor $B(\alpha, \Omega_{nb}/\Omega_b) = \delta_k/\Delta_k$ in the small wavelength limit, $k_p \gg m_{v,s}$, as a function of force strength α , for various values of Ω_{nb}/Ω_b : solid curve 0.95/0.05; short-dashed, 0.9/0.1; long-dashed, 0.8/0.2 and dashed-dotted curve, 0.7/0.3.
- 4) Schematic modification of the transfer function for adiabatic density perturbations, $F(k)$, due to a repulsive (solid line) or attractive (dashed line) long-range force; $q = \frac{3p}{2} - 1$, where p is given by eq. (3.12) or (3.13). A fluctuation with $k < k_n$ ($k > k_n$) has never (always) been subject to the additional long-range force.
- 5) Present linear power spectrum as a function of wavelength, for various values of α . The solid line represents the spectrum of the spatially flat CDM model with scale-invariant primordial fluctuations (Davis *et al.* 1985), our 'reference model'. The short-dashed curve shows the power spectrum with an additional interaction of range $\lambda = 10$ Mpc; short-long dashed curve, $\lambda = 1.3$ Mpc; long-dashed curve, $\lambda = 100$ kpc; and dashed-dotted curve, $\lambda = 10$ kpc.
- 6) Spatial two-point mass correlation function, $\xi(r)$, for repulsive forces of various ranges, λ . The curves have the same meaning (correspond to the same values of λ) as in fig. 5; here, the dashed-dotted curve shows the power-law $\xi(r) = (r/r_0)^{-1.8}$ with $r_0 = 5.6 h^{-1} Mpc$ ($h=1/2$). a) Force strength $\alpha = -0.5$; b) $\alpha = -0.3$.
- 7) Galaxy angular correlation function, $w(\theta)$, for repulsive force of strength $\alpha = -0.3$ and the same values of the range λ as in fig. 5, at the depth corresponding to the

magnitude limit of the APM survey. The data are from the APM (filled circles) and second Palomar Sky surveys. The APM intraplate data, which does not require interplate corrections, is shown separately by the unfilled circles. The POSS-II data for the northern (filled squares) and southern (crosses) skies are also shown individually.

- 8) Expected rms bulk velocity $v_{rms}(r)$ for various values of force strength, α , and range, λ (curves are λ -coded as in fig. 5), averaged with a Gaussian window function. The dashed-dotted curve ($\lambda = 10$ kpc) coincides with the standard CDM model. We also include the fitted large-scale streaming velocity of 600 ± 100 km/sec (Dressler *et al.* 1987), and the smaller value of 570 ± 60 km/sec from the "Great Attractor" model (Lynden-Bell *et al.* 1988).
- 9) Average large-scale streaming velocity $u(r)$ defined with a top-hat selection function and additional (Gaussian) smoothing on scale $r_s = 12 h^{-1}$ Mpc. Different curves represent different force ranges λ (as in fig. 5). The two data points indicate the bulk flow from the reconstructed velocity field (Bertschinger *et al.* 1990): 388 ± 67 km/sec and 327 ± 82 km/sec on scales 80 Mpc and 120 Mpc (with $h = 1/2$).
- 10) Cosmic Mach number for different parameters α and ranges λ (as in fig. 5). The two data points indicate the observational estimates from spiral and elliptical galaxy samples (see text).
- 11) Temperature auto-correlation function on angular scale θ for various values of α and λ (as in fig. 5). The shaded area indicates the region excluded by COBE measurements (Smoot *et al.* 1991), $C(\theta) < 1.0 \cdot 10^{-9}$ in the range $15^\circ \leq \theta \leq 165^\circ$.
- 12) The quadrupole moment of the CMBR anisotropy as a function of force strength α . Different curves correspond to different values of λ (as in fig. 5). The shaded area represents the experimental limit from RELIKT (Strukov *et al.* 1987) and COBE (Smoot *et al.* 1991), $C_2^{1/2} < 3 \cdot 10^{-5}$ at 95 % confidence level.

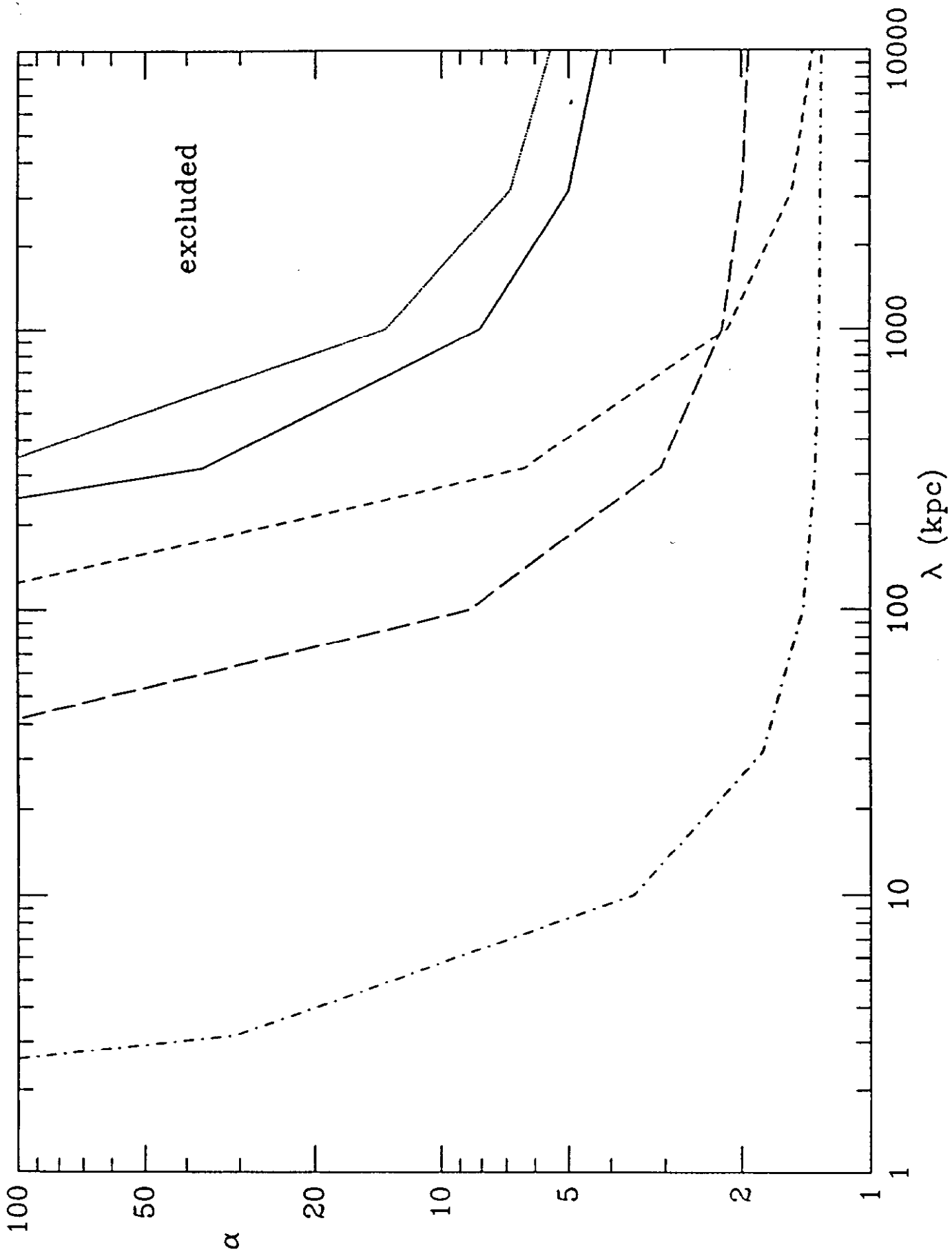


Fig. 1

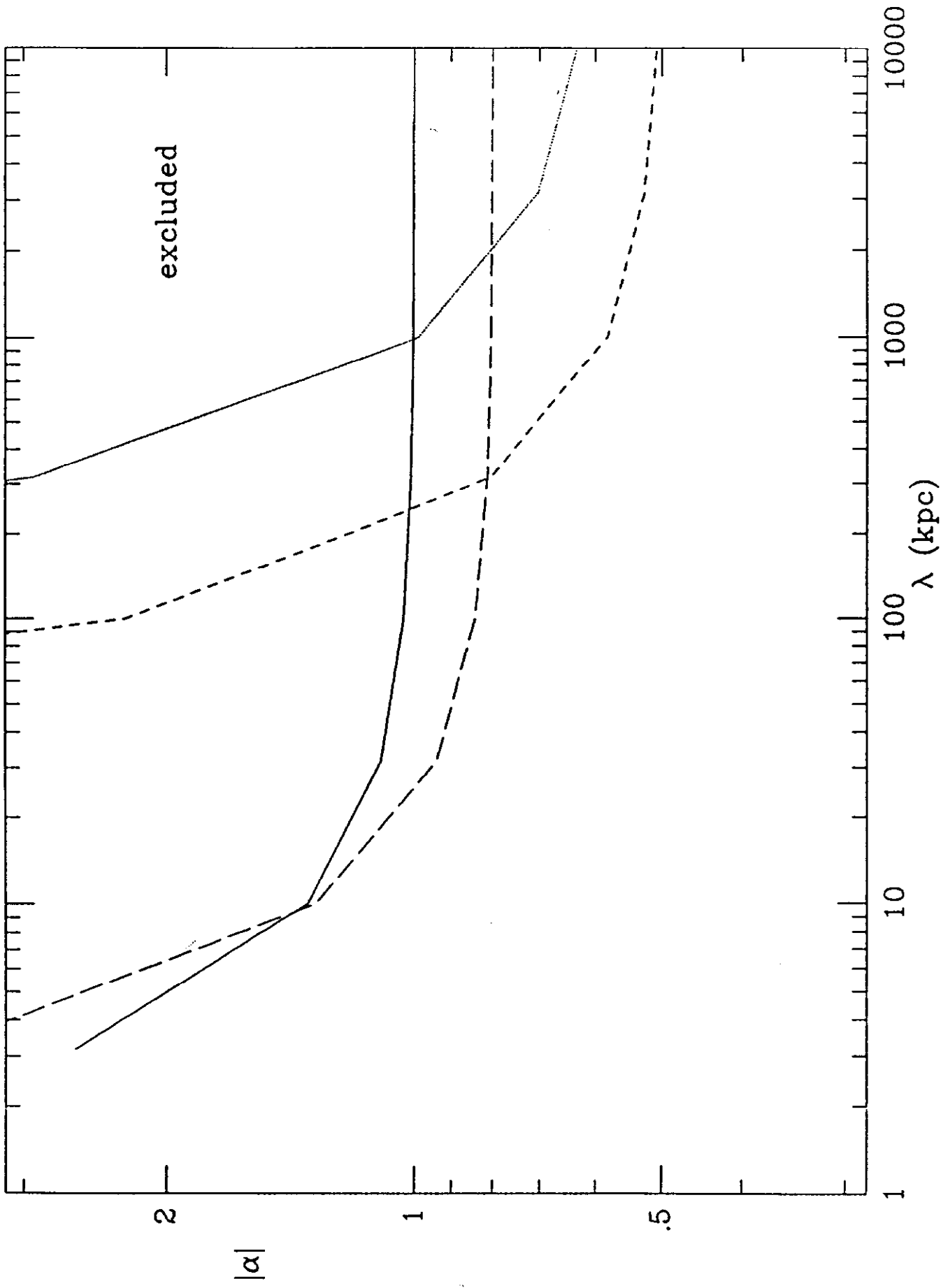
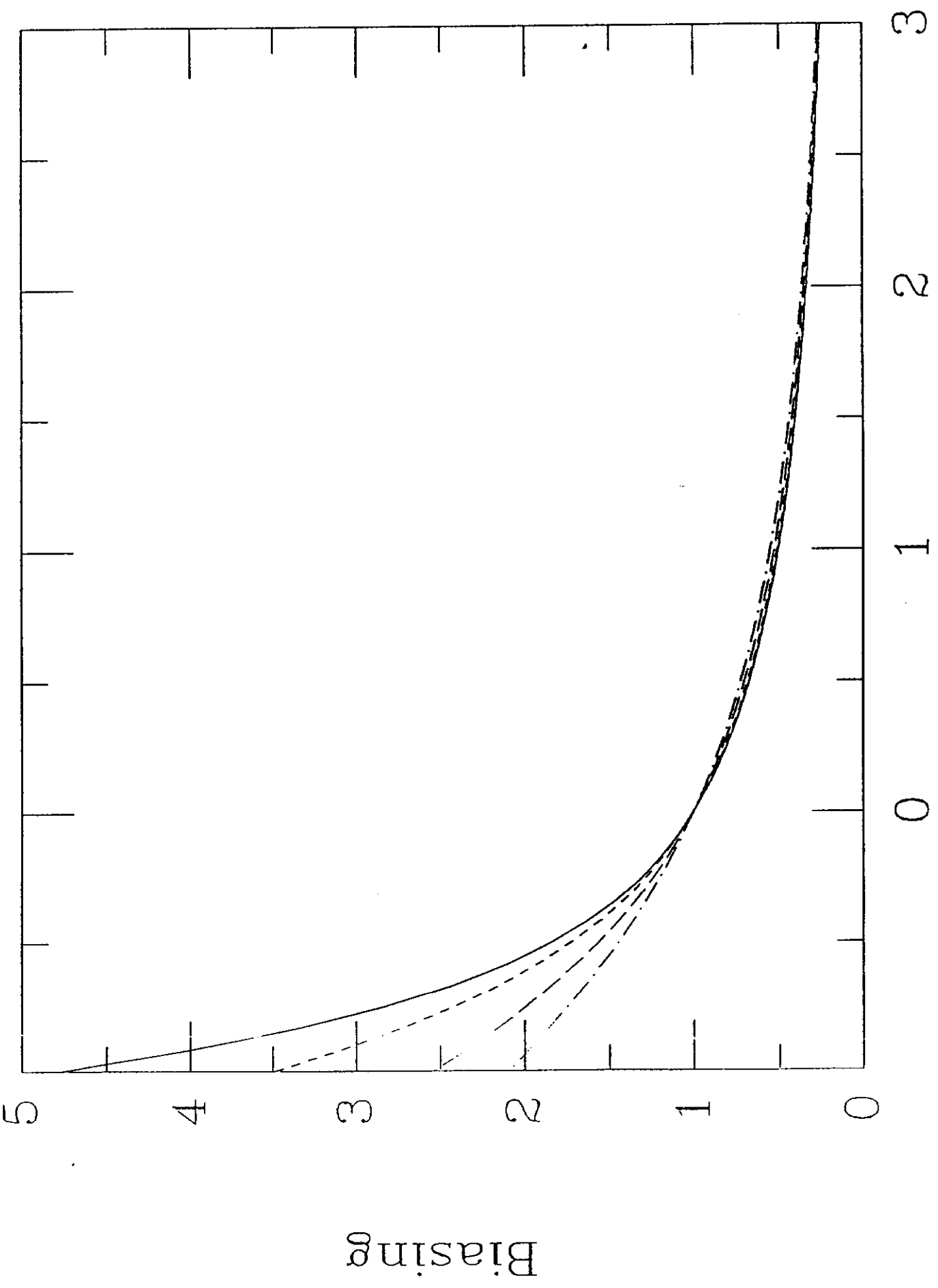


Fig. 2

Fig. 3



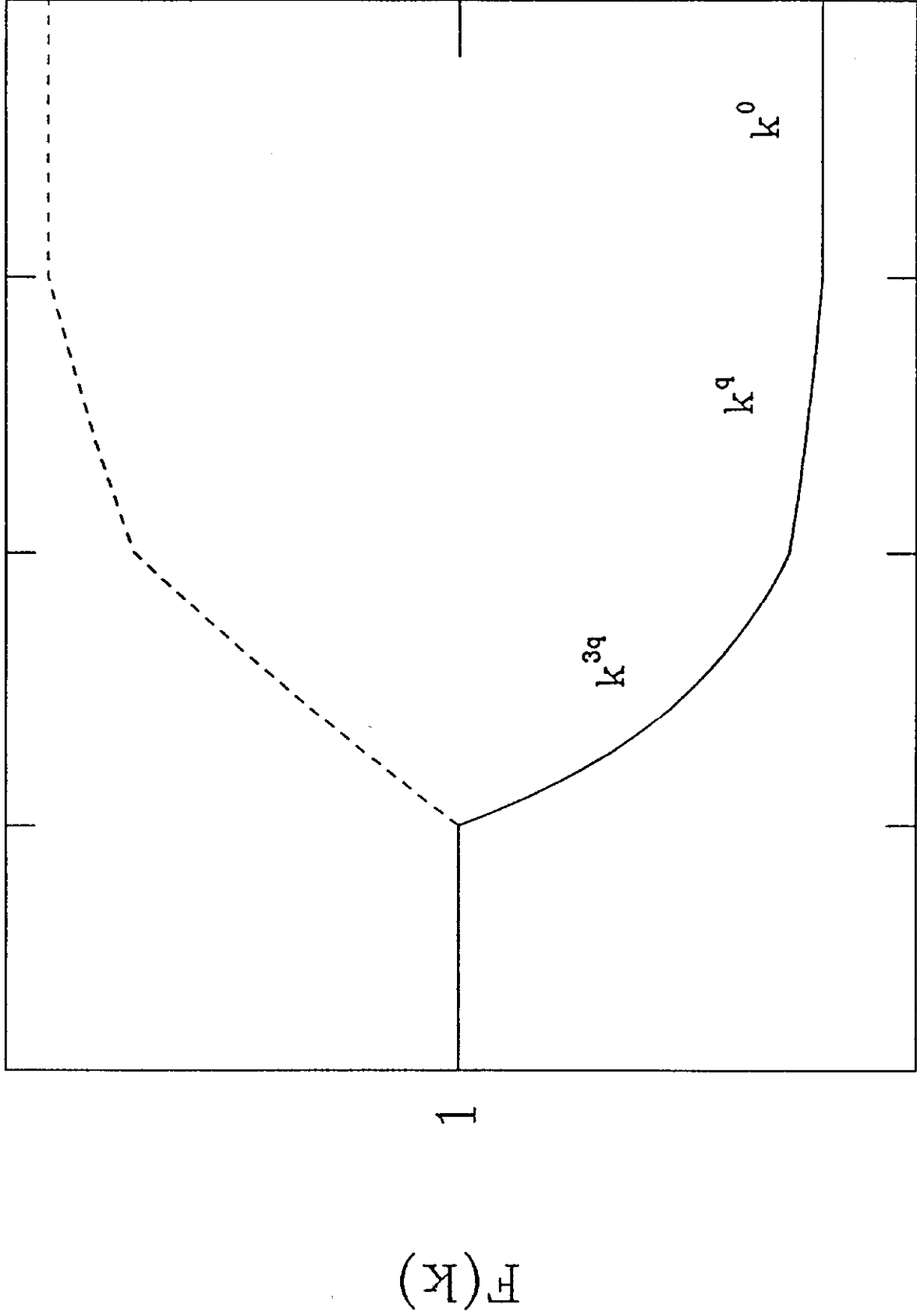


Fig. 4

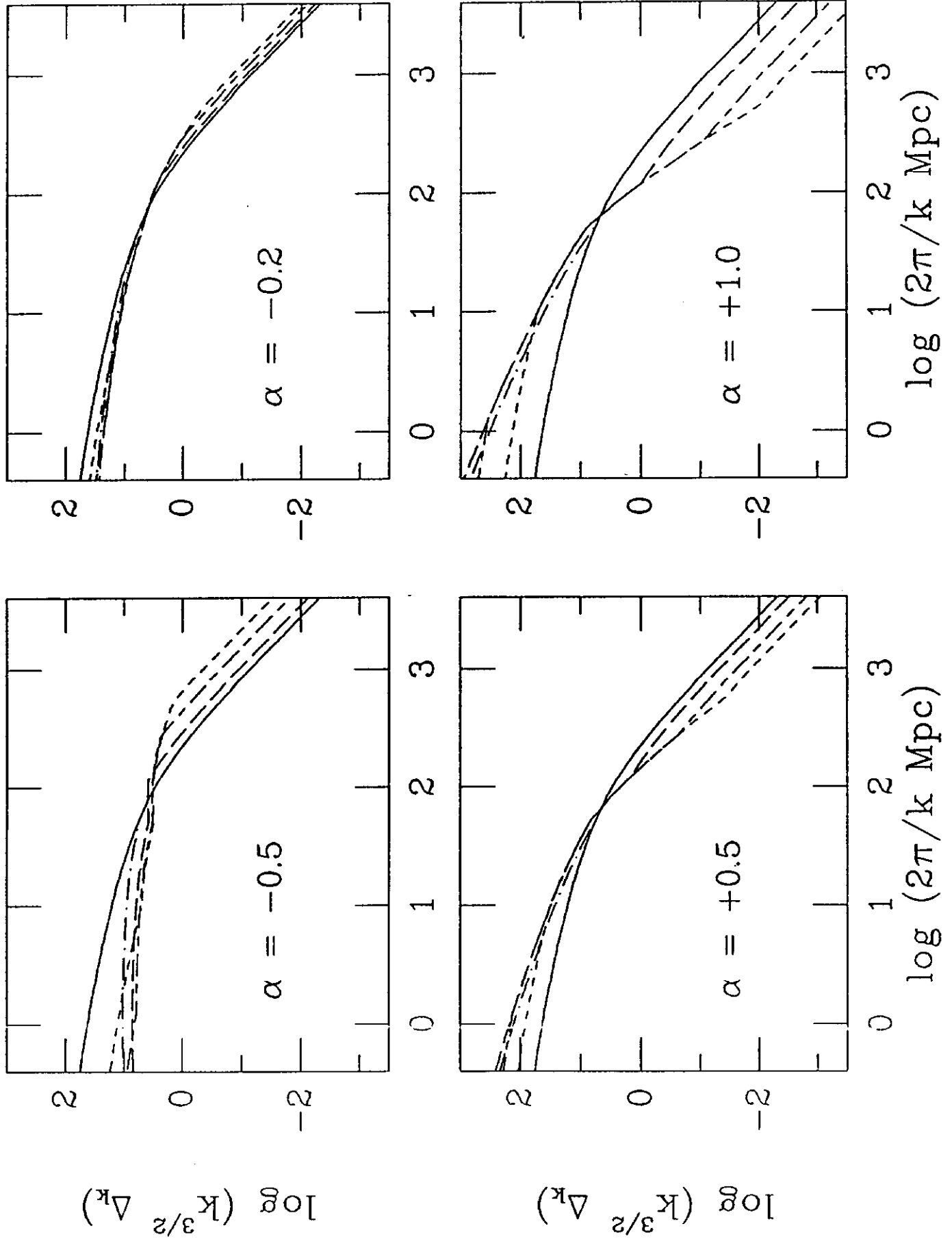


Fig. 5

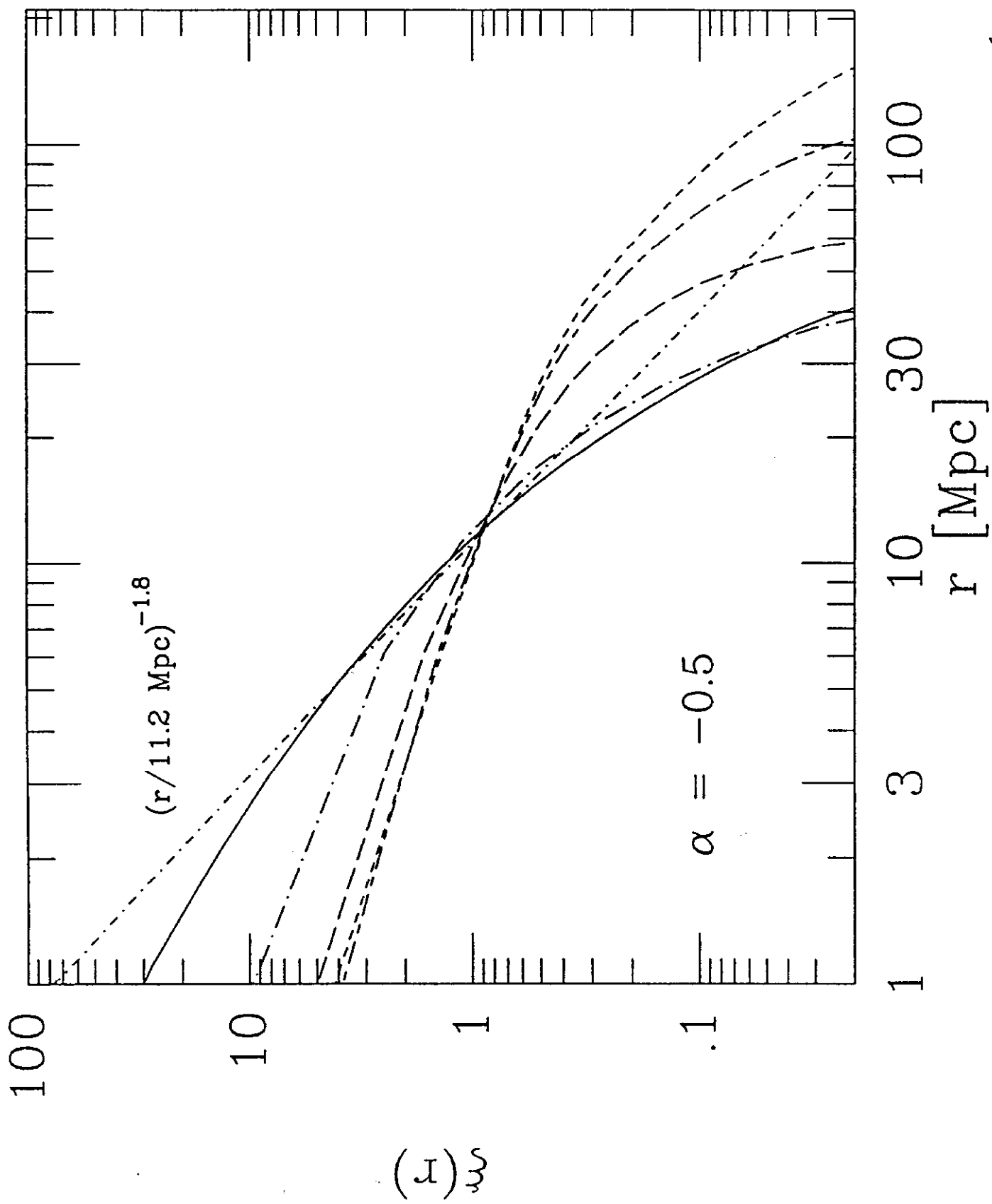


Fig. 6a.)

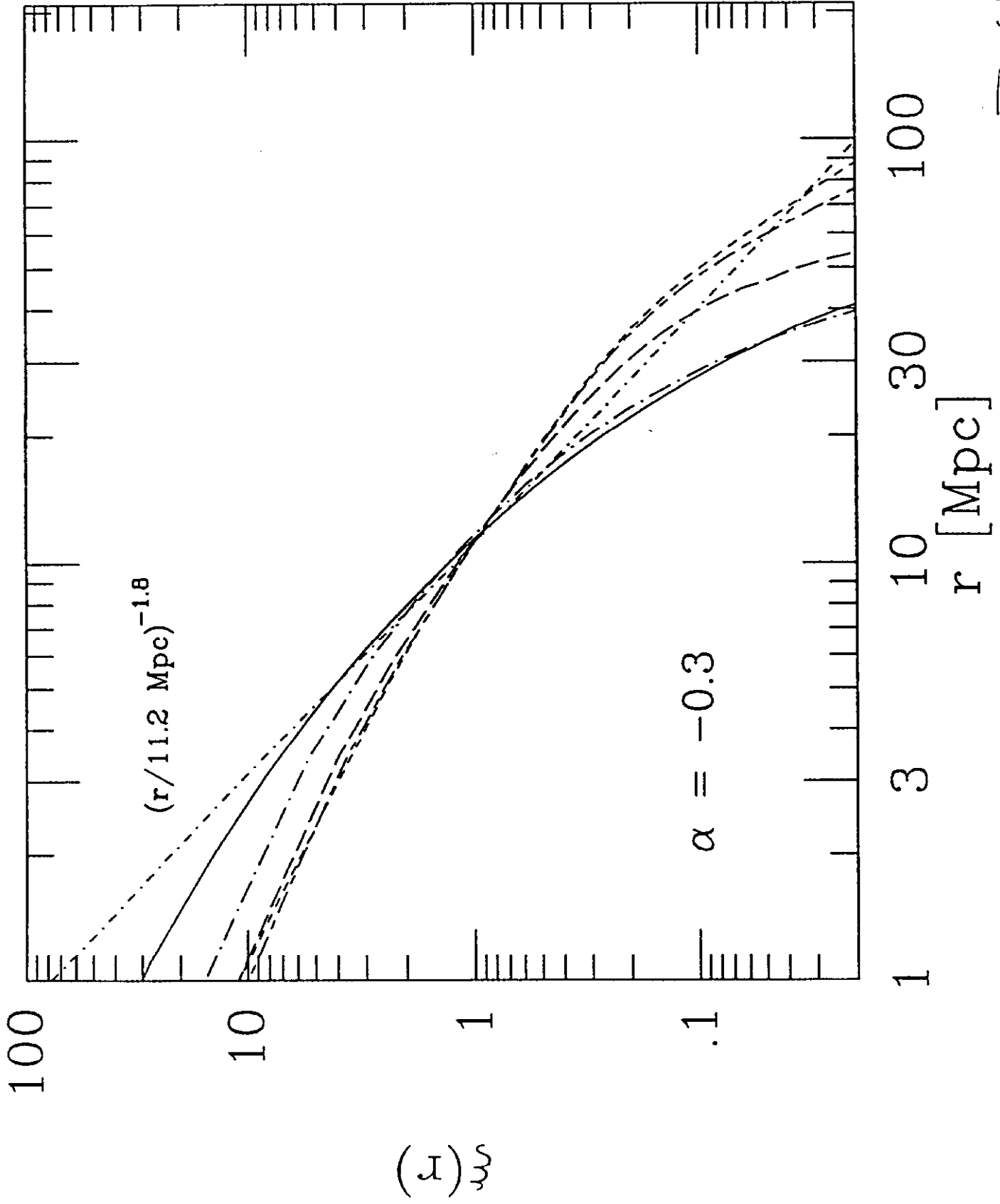


Fig. 6 b.)

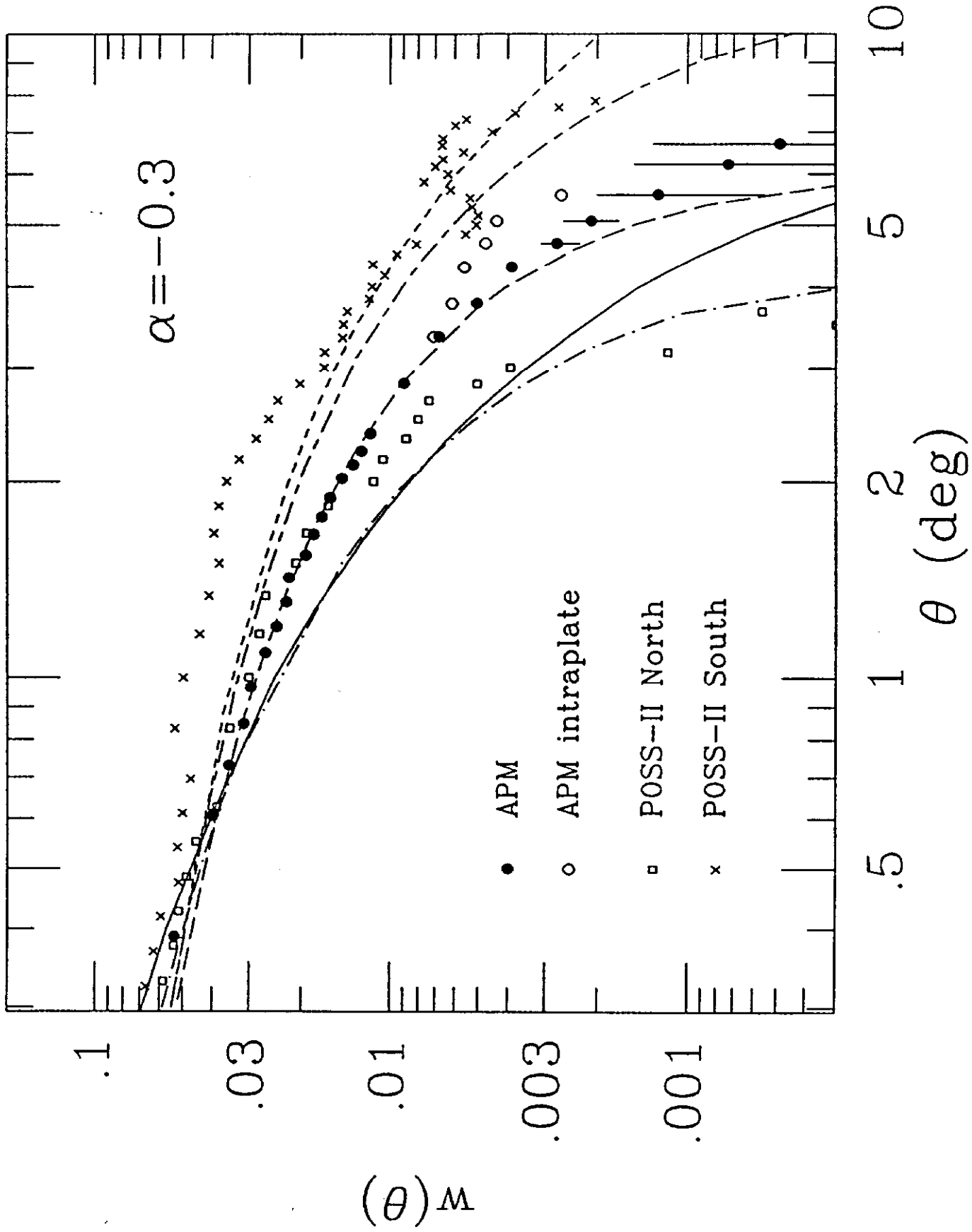


Fig. 7

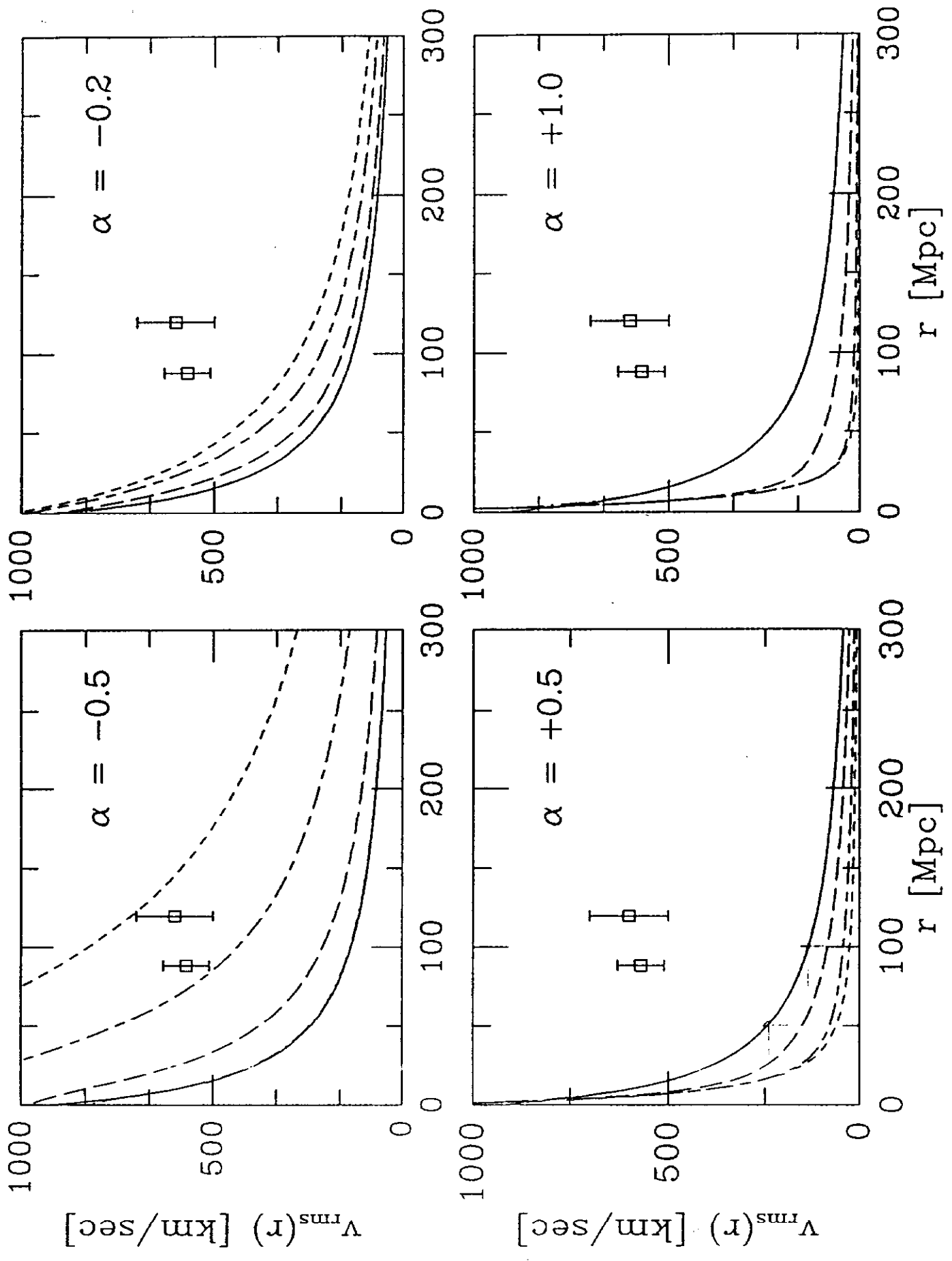


Fig. 8

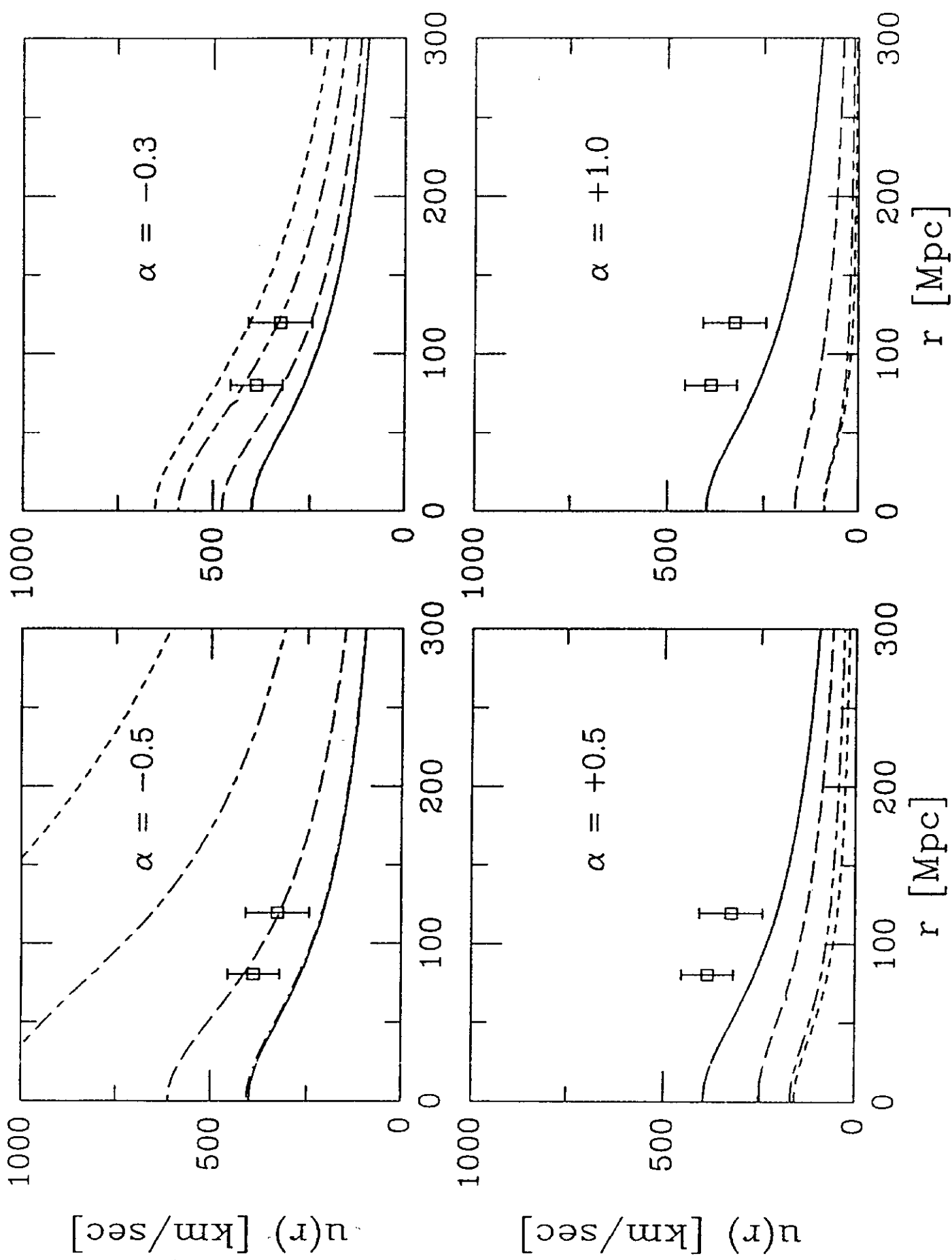


Fig. 9

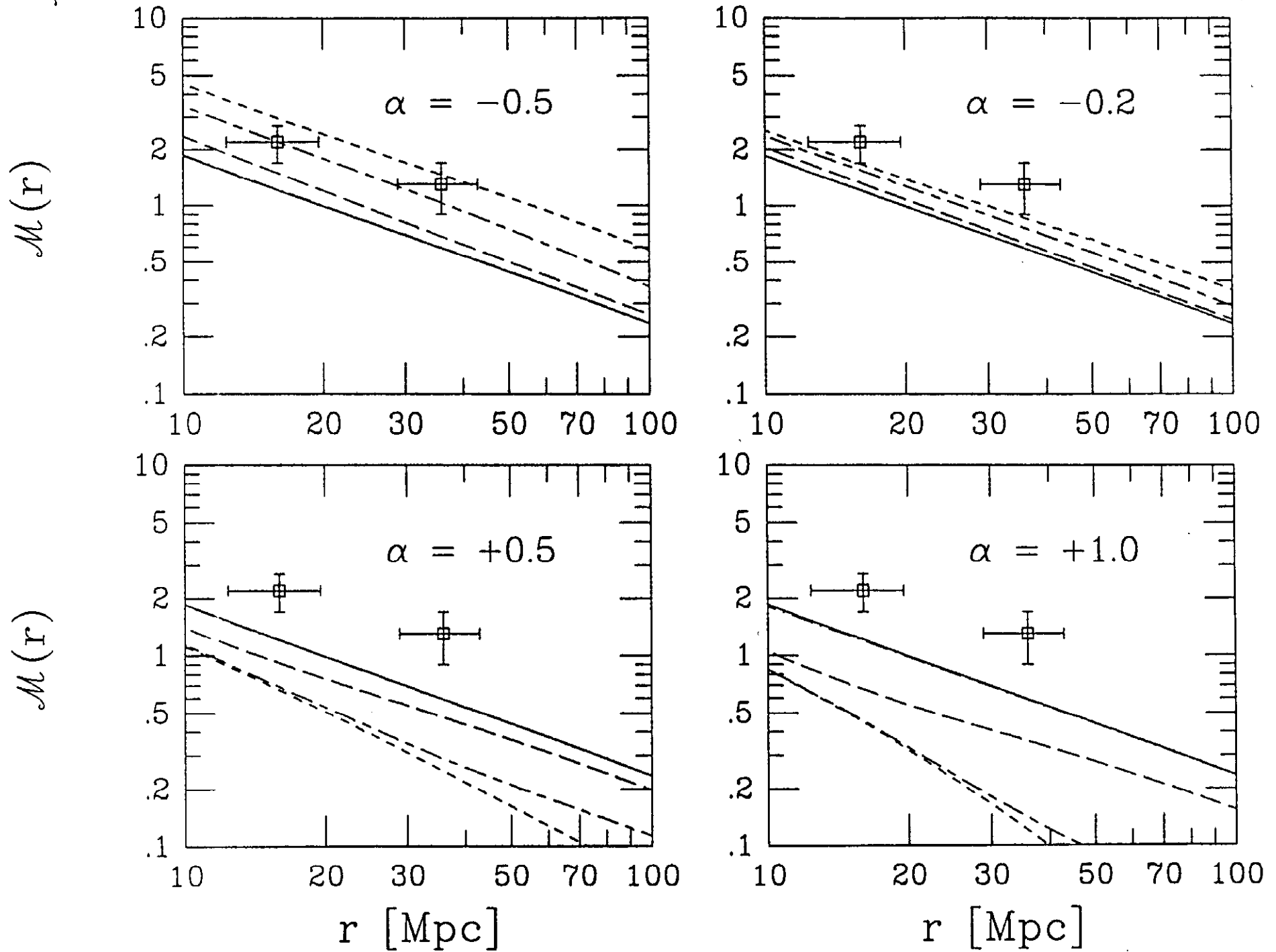


Fig. 10

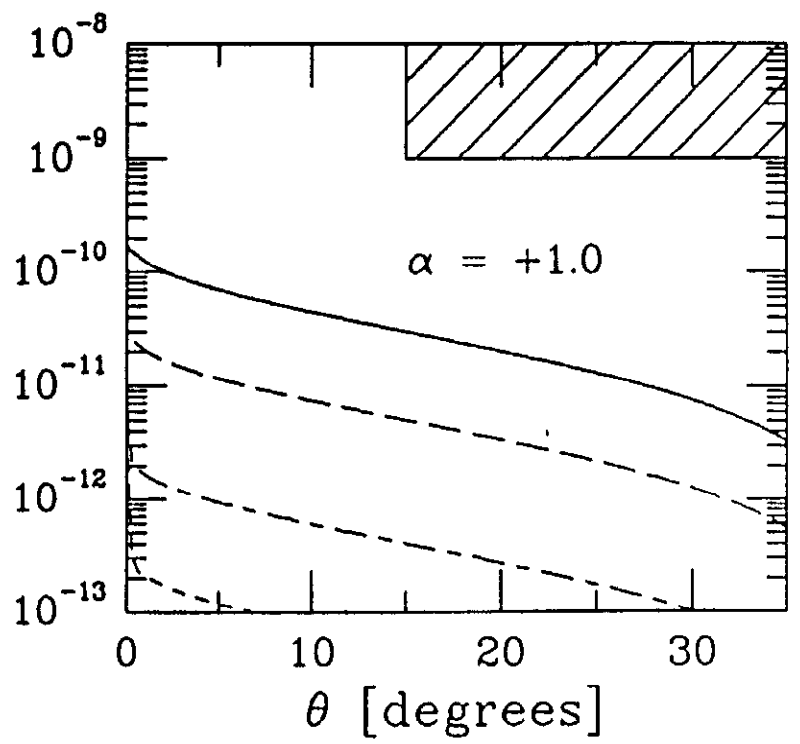
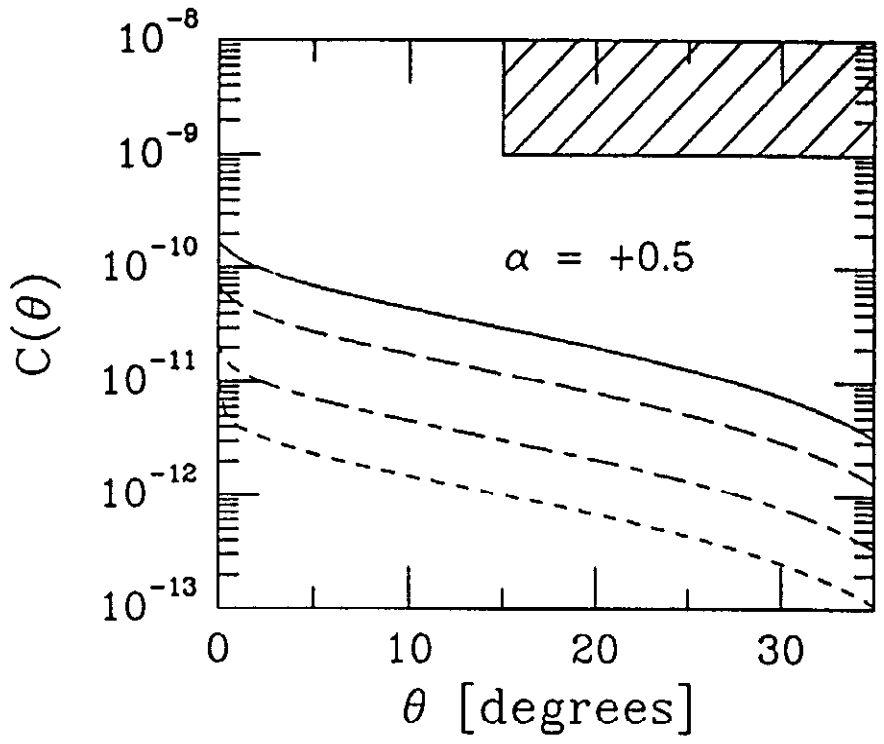
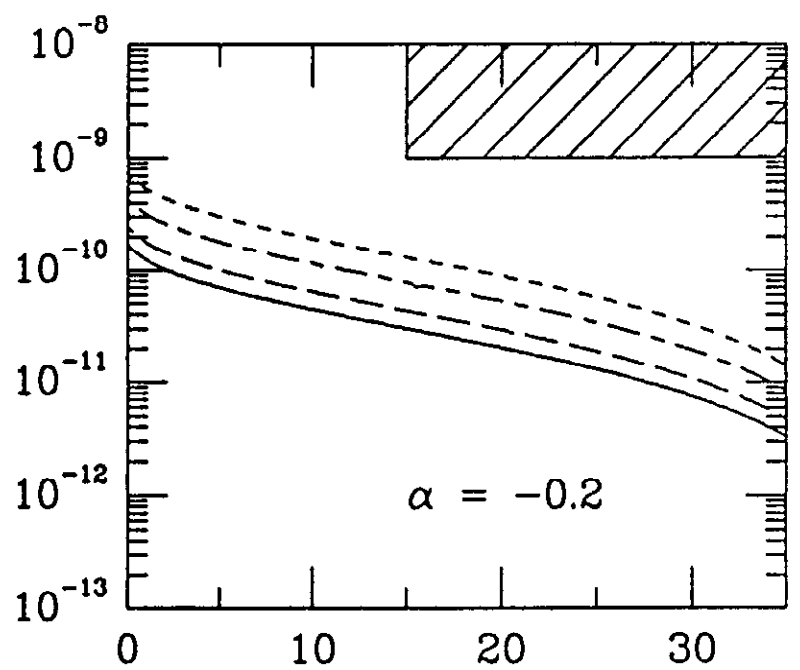
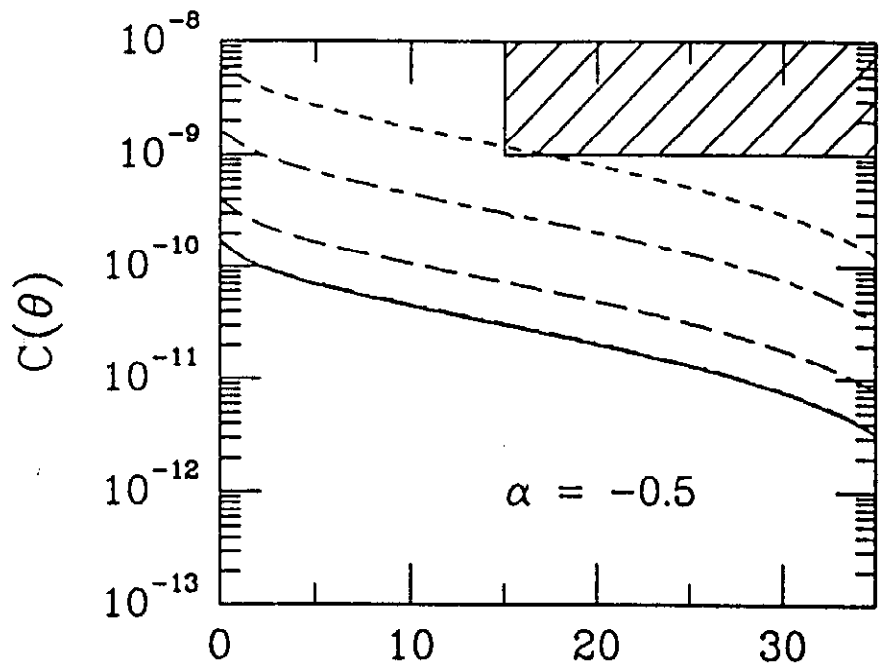


Fig. 11

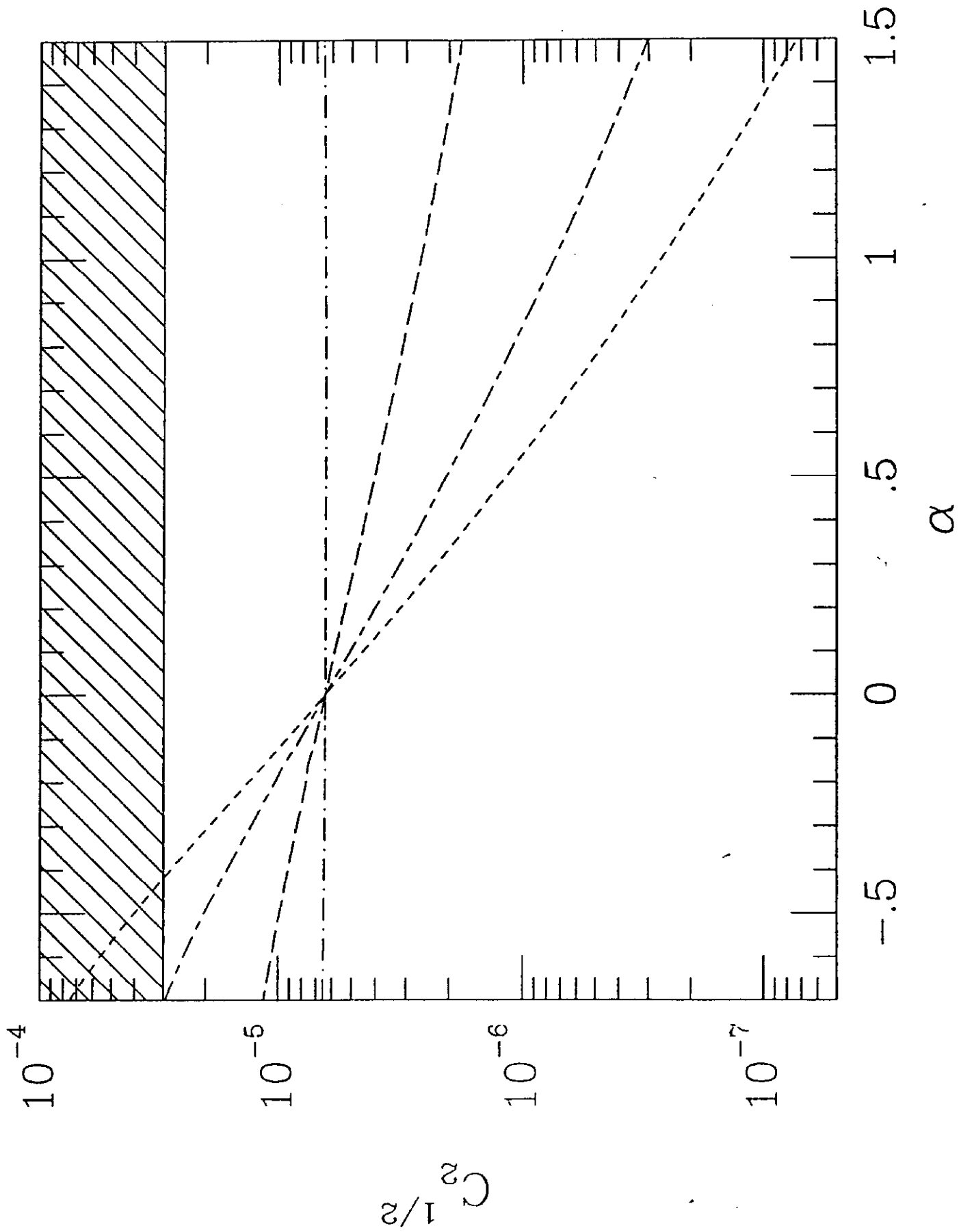


Fig. 12